

The Pennsylvania State University

The Graduate School

Department of Energy and Mineral Engineering

**DETERMINATION OF CRICONDENTHERM,  
CRICONDENBAR AND CRITICAL POINTS OF NATURAL GASES  
USING ARTIFICIAL NEURAL NETWORKS**

A Thesis in

Petroleum and Mineral Engineering

by

Yunusa A Abass

Submitted in Partial Fulfillment  
of the Requirements  
for the Degree of

Master of Science

December 2009

The thesis of Yunusa A. Abass was reviewed and approved\* by the following:

Luis F. Ayala  
Assistant Professor of Petroleum and Natural Gas Engineering  
Thesis Advisor

Zuleima T. Karpyn  
Assistant Professor of Petroleum and Natural Gas Engineering  
Department of Energy and Mineral Engineering

Turgay Ertekin  
Professor of Petroleum and Natural Gas Engineering  
George E. Trimble Chair in Earth and Mineral Engineering  
Program Chair in Petroleum and Mineral Engineering

Yaw D. Yeboah  
Professor and Department Head of Energy and mineral Engineering

\*Signatures are on file in the Graduate School

## ABSTRACT

A phase envelope is a diagram which characterizes fluid behavior at different pressures and temperatures, and also shows the conditions at which liquid and vapor phases coexist. To be able to fully characterize this behavior, it is of utmost importance that we are able to trace the fluid's critical point (location of the condition where liquid and vapor phases become indistinguishable), cricondentherm (corresponding value of the highest temperature of Liquid/Vapor coexistence) and cricondenbar (corresponding values of the highest pressure of Liquid/Vapor coexistence) located within its phase envelope. These three points are the most important ones in terms of defining the shape of the envelope. Thus, in order to be able to determine the shape of phase envelope, we should be able to accurately predict the location of the critical temperature and pressure along with the cricondentherm's and cricondenbar's temperature and pressure. This, among others, will aid our understanding of the production characteristics of the hydrocarbons present in the reservoir. In this work, Artificial Neural Networks are used to aid in this prediction. This study presents an expert system which is capable of understanding the complexities of the relationship between the composition and the corresponding values of the key points on the phase envelope. The expert system is able to predict the most relevant input among the compositional data of the reservoir fluid. A four stage neural network was proposed and it was found that, when compared with other constituents that make up the hydrocarbon mixture, the most relevant and consistent of all the input compositional data used in the neural network prediction of the phase envelope, was the  $C_{7+}$  for all the stages examined.

## TABLE OF CONTENTS

LIST OF FIGURES .....	v
LIST OF TABLES .....	viii
NOMENCLATURE .....	viii
ACKNOWLEDGEMENTS .....	x
Chapter 1. Introduction .....	1
Chapter 2. Background .....	3
2.1 Phase Envelope Calculations .....	8
2.1.1 Phase Envelope Construction .....	9
2.2 Critical, Cricondenbar and Cricondentherm Calculations .....	18
2.3 Artificial Neural Network .....	26
2.3.1 Backpropagation Learning .....	29
Chapter 3. Problem Statement .....	33
Chapter 4. ANN Model Development .....	35
4.1 Phase Envelope Neural Network Data .....	38
4.1.1 Neural Network Model .....	41
Chapter 5. Results .....	48
5.1 Stage One-Cricondenbar, Cricondentherm and Critical Network Models .....	49
5.1.1 Cricondenbar Neural Network .....	50
5.1.2 Cricondentherm Neural Network .....	55
5.1.3 Critical Neural Network .....	60
5.2 Stage Two-3-Coordinate Neural Network .....	64
Chapter 6. Summary and Conclusion .....	73
Bibliography .....	76
Appendix A: Stage 1 ANN MATLAB Code Cricondenbar .....	82
Appendix B: Phase Envelope Code for MATLAB Stage Two .....	88

## LIST OF FIGURES

Figure 2-1: Typical phase envelope of a reservoir fluid .....	5
Figure 2-2: Phase envelope of the various types of reservoir fluids (after Pedersen and Christensen). .....	7
Figure 2-3: Phase envelope showing cricondentherm, cricondenbar and critical point .....	9
Figure 2-4: Neural network with three layers .....	27
Figure 4-1: $C_1$ Ranges for Training and Testing.....	38
Figure 4-2: Sample of various envelopes showing distribution of pressure and temperature values .....	44
Figure 4-3: Testing and Training Data for Cricondenbar Network Model.....	45
Figure 4-4: Testing and Training Data for Cricondentherm Network Model .....	45
Figure 4-5: Testing and Training Data for Critical Network Model .....	45
Figure 4-6: Ranges for the Temperature-Pressure 3-Coordinate Network Model .....	48
Figure 5-1: Neural Network Architect for Cricondenbar's Training and Testing .....	50
Figure 5-2: Training (left) and Testing (right) Result Plots for the Normalized Pressure of Cricondenbar Points.....	51
Figure 5-3: Training (left) and Testing (right) Result Plots for the Normalized Temperature of Cricondenbar Points.....	52
Figure 5-4: Relevancy for each input for Cricondenbar .....	54
Figure 5-5: Neural Network Architect for Cricondentherm's Training and Testing ..	56
Figure 5-6: Training (left) and Testing (right) Result Plots for the Normalized Pressure of Cricondentherm Points .....	59
Figure 5-7: Training (left) and Testing (right) Result Plots for the Normalized Temperature of Cricondentherm Points.....	58
Figure 5-8: Relevancy percentage for the Cricondentherm neural network.....	59
Figure 5-9: Architect for the Critical Neural Network .....	60

Figure <b>5-10</b> : Training (left) and Testing (right) Result Plots for the Normalized Pressure Points of Critical Points .....	61
Figure <b>5-11</b> : Training (left) and Testing (right) Result Plots for the Normalized Temperature of Critical Points.....	62
Figure <b>5-12</b> : Relevancy percentage for the critical neural network.....	63
Figure <b>5-13</b> : Phase Envelope Neural Network Architect .....	64
Figure <b>5-14</b> : 3-Coordinate Cricondenbar Training (left) and Testing (right) Pressure Results Plots.....	66
Figure <b>5-15</b> : 3-Coordinate Cricondenbar Training (left) and Testing (right) Temperature Results Plots .....	67
Figure <b>5-16</b> : 3-Coordinate Cricodentherm Training (left) and Testing (right) Pressure Results Plots.....	68
Figure <b>5-17</b> : 3-Coordinate Cricodentherm Training (left) and Testing (right) Temperature Result Plot .....	69
Figure <b>5-18</b> : 3-Coordinate Critical Training (left) and Testing (right) Pressure Result Plot.....	70
Figure <b>5-19</b> : 3-Coordinate Critical Training (left) and Testing (right) Temperature Result Plot.....	71
Figure <b>5-20</b> : Relevancy Plot for the Phase Envelope Input.....	72

**LIST OF TABLES**

Table 4-1: Phase envelope input data range .....	37
Table 4-2: Phase envelope possible actual values used for training.....	37
Table 4-3: $P_N$ and $T_N$ Range for Cricondenbar Neural Network .....	43
Table 4-4: $P_N$ and $T_N$ Range for Cricodentherm Neural Network .....	43
Table 4-5: $P_N$ and $T_N$ Range for Critical Neural Network.....	43

**NOMENCLATURE**

P	pressure, psia
T	temperature, °R
$P_N$	normalized pressure i.e. reduced pressure value
$T_N$	normalized temperature i.e. reduced temperature value
$P_b$	bubble point pressure
$R_s$	solution gas to oil ratio SCF/STB
$x_i$	liquid fraction
$y_i$	vapor fraction
$z_i$	mole fraction of component in mixture
$P_c$	critical pressure, psia
$T_c$	critical temperature, °R
MW	molecular weight, lb/lbmol
SG	specific gravity
$C_1$	methane
$C_2$	ethane
$C_3$	propane
$C_4$	butane
$C_5$	pentane
$C_6$	hexane
$C_{7+}$	heptanes-plus
$N_2$	nitrogen

$H_2S$	hydrogen sulfide
$CO_2$	carbon dioxide
$n$	total number of component
$T_t$	cricondenthem temperature
$T_p$	cricondenbar temperature
$P_t$	cricondenthem pressure
$P_p$	cricondenbar pressure

**Greek**

$\gamma$	specific gravity, at (60°F/60°F)
$\omega$	acentric factor
$\Phi_i^v$	fugacity coefficient of component i in vapor phase
$\Phi_i^l$	fugacity coefficient of component i in liquid phase

**Abbreviation**

PVT	pressure-volume-temperature
VLE	vapor-liquid equilibrium
EOS	equation of state
PR	Peng-Robinson
SRK	Soave- Redlich-Kwong
ANN	artificial neural network
LMS	least mean square

## ACKNOWLEDGEMENTS

First and foremost, to the Almighty Allah is the glory. This thesis could not have been without the support and guidance of my thesis Advisor Dr Luis Ayala. I would like to express my deepest regard and gratitude to him for his guidance and assistance throughout the pursuit of my diploma and most especially this thesis work. I would also like to express my deep appreciation to Dr Turgay Ertekin for his guidance and assistance towards this work. My thanks also goes to Dr Zuleima Karpyn for her interest in serving on my research committee.

I also owe a great deal of appreciation to my entire family, without them there would be no me. Words cannot express how much I appreciate the encouragement and support from everyone of them and most especially to my wonderful son Tahmid Abass.

To my colleagues, Shakirundeen Omofolarin Shakioye, Adewale Monsur Olatunji, Olayanju Cole, Gurpreet Singh, Armstrong Lee Agbaji, Burak Kulga and Mohammed Ojogbane, your friendship was a guiding grace for me.

And finally the entire staff of the College of Earth and Mineral Science, Department of Energy and Mineral Engineering, I am forever grateful.

## **Chapter 1**

### **Introduction**

Petroleum reservoir fluids contain a variety of substances of diverse chemical nature that include hydrocarbons and non-hydrocarbons. Hydrocarbons (carbon-hydrogen molecules) range from methane to asphalt. Non-hydrocarbons include substances such as nitrogen, carbon dioxide, and sulfur compounds. Hydrocarbons are the main constituents of petroleum reservoir fluids and they have a very complex chemistry. The behavior of hydrocarbon mixtures primarily depends on their chemical composition and the prevailing temperature and pressure at both the reservoir and the surface conditions. These hydrocarbons in most cases exist naturally in more than one phase - liquid, vapor and/or solid.

While a phase diagram is a pictorial representation of the distinction between these phases, a phase envelope is a region on a phase diagram that is bounded by a line which encompasses where two phases can coexist. These lines on the phase envelope are known as the bubble point and the dew point lines. These two lines are joined together at a point known as the critical point. The point corresponding to the highest pressure value on the phase envelope is known as the cricondenbar while the point corresponding to the highest temperature is known as the cricondentherm. These three points help in defining the characteristics of the phase envelope of any particular reservoir fluid. Phase envelopes are very critical in our understanding of the reservoir fluids, their initial thermodynamic

state at conditions of discovery, and our ability to predict reservoir fluid changes as pressure and temperature conditions vary during the reservoir's productive life. This knowledge is critical in properly and effectively designing best production practices for every type of reservoir fluid. In general, prediction of reservoir depletion behavior heavily relies on being able to account for the state at which the reservoir fluid is at any conditions of pressure and temperature.

This study proposes a method for phase envelope prediction based on the estimation of key points associated with the fluid's envelope. In order to achieve this, neural network technology is implemented in this study in order to understand the complexities of the relationship between the input variables and output variables associated with typical phase envelopes of natural gas reservoirs. These input variables are the compositions of natural gas which are: methane  $C_1$ , ethane  $C_2$ , propane  $C_3$ , butane  $C_4$ , pentane  $C_5$ , hexane  $C_6$ , heptanes  $C_{7+}$ , hydrogen sulfide  $H_2S$ , nitrogen  $N_2$ , and carbon dioxide  $CO_2$ . Other input variables include molecular weight of the  $C_{7+}$  ( $MW C_{7+}$ ) and specific gravity of  $C_{7+}$  ( $SG C_{7+}$ ). These would generate the corresponding temperature and pressure values of the critical point, cricondenbar and the cricondentherm of the phase envelope. This study also investigates which of the input variable is most relevant in determining the phase envelope's characteristics by using a relevancy analysis of the proposed network.

## **Chapter 2**

### **Background**

Multicomponent mixture characterizations of reservoir fluids which exist as complex hydrocarbons are important to petroleum processes in order to be able to provide accurate fluid description, present solutions to improve compositional analysis and aid in system design. It is also a basis for the economics of projects with accurate phase behavior predictions as a major objective.

A phase is defined as a homogeneous and physically distinct part of a system which is separated from the other parts. The different phases which occur either naturally or induced is depicted by a phase diagram. A phase diagram is required to properly define these multicomponent mixtures of hydrocarbon. Phase behavior studies the different phase change (i.e. liquid, vapor and/or solid) which occur between these multicomponent mixtures of hydrocarbon as a function of temperature, pressure and composition. Each hydrocarbon system has its own phase diagram, which depends on the composition of the system. Hydrocarbon systems are mostly found during petroleum production in liquid phase as oil, distillate or condensate, as vapor or gas phase in form of natural gas. They can also be found in the solid phase as paraffin or other forms of deposit which occur in the tubing system or in the surface production facilities as gas hydrates due to the freezing and distortion in gas flow through the lines and sand as sediments from the reservoir rock particles.

The subject of phase behavior focuses on when these phases are in equilibrium, at which no changes occur in the system with time (i.e. if the system is left at the same temperature

and pressure). At equilibrium, evaporation and condensation processes are exactly balanced and there is no net change in the mass of either phase. This phase equilibrium state must also be satisfied by thermal, mechanical and chemical equilibrium conditions. In most petroleum engineering applications, the general assumption is that the fluids which exist in the reservoir are in equilibrium. Essentially phase equilibrium calculation is a very important aspect of the general difficulty of constructing a fluid behavior in terms of pressure-composition, pressure-temperature, composition-composition (ternary), temperature-composition and pressure-volume diagrams.

A phase diagram of a multicomponent mixture has a region bounded by a line where two phases exists in equilibrium. This bounded region is known as a phase envelope, a saturation envelope or the two phase region. A phase envelope shows the boundaries between a single and the two phase region for a multicomponent mixture at equilibrium conditions. These lines are known as the bubble point line and the dew point line. They meet at the critical point of the mixtures on pressure (P) and temperature (T) plot. Fig **2.1** shows a typical phase envelope for a reservoir fluid where the liquid is found to the left of the bubble line and the vapor region is found to the right of the dew point line. At the bubble point line where the mixture is found to be in liquid with incipient amount of gas, this liquid at this point is said to be saturated. On the other hand, on the dew point line where the mixture is found to be in vapor form with a slight amount of liquid, the gas at this stage is said to be saturated.

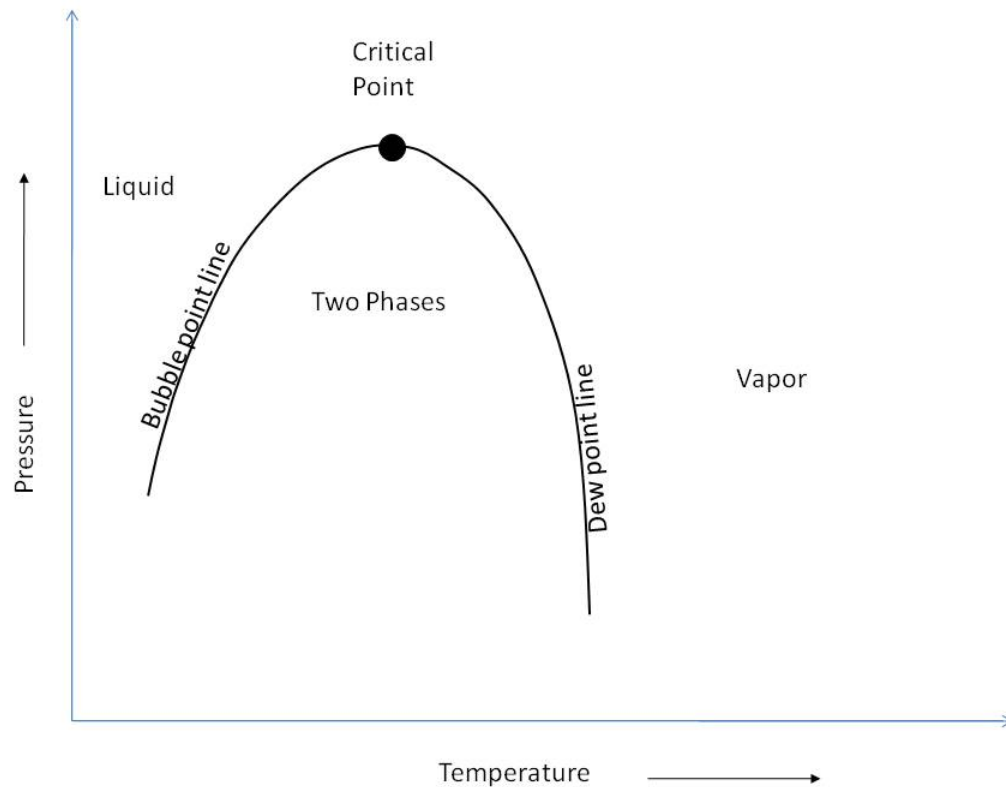


Figure 2-1: Typical phase envelope of a reservoir fluid

Phase envelopes are instrumental in the classification of reservoirs, classifying the naturally occurring hydrocarbon systems and also used to describe the characterizations of phase diagrams of the reservoir fluid. A reservoir classification is based on the relative location of the initial reservoir temperature ( $T_i$ ) and pressure ( $P_i$ ) with respect to the reservoir's fluid phase envelope. This groups reservoirs into two types of hydrocarbon reserves which are either a natural gas or oil reservoirs. A reservoir is classified as a natural gas reservoir if its temperature is higher than the fluid critical temperature. While it is classified as an oil reservoir if its temperature is lower than the fluid critical

temperature. Due to the wide range of the physical and chemical properties associated with hydrocarbon reservoirs, oil reservoirs are further classified into three main types of reservoirs. These are: undersaturated oil reservoir, saturated oil reservoir and the gas-cap reservoir. Gas reservoirs on the other hand are grouped into four main classes namely, retrograde gas-condensate reservoir, near-critical gas condensate, wet gas reservoir and dry gas reservoir.

Phase envelopes are also essential for identifying the various types of reservoir fluids. Reservoir fluids are classified into five main groups, namely: dry gas, wet gas, gas condensate, volatile oil and black oil. These are the most commonly identified petroleum reservoir fluids. A phase envelope comes as a very useful diagram when identifying which class a reservoir fluid belongs. The various types of reservoir fluids are distinguished by the relative location of the mixture's critical temperature point to the reservoir initial temperature as shown in Fig 2.2. Reservoir fluids are also identified by conditions and locations of the critical temperature and the cricondentherm (highest temperature) on the phase envelope with the initial reservoir condition. The reservoir depletion paths are very important in further understanding the characteristics of these fluids i.e. when a reduction in the temperature and pressure conditions occurs due to production. For a dry gas the reduction in pressure and temperature conditions has no impact on the number of phases that will occur during the reservoir depletion path as well as surface depletion path. A wet gas also does not produce two phases during its depletion but is more likely to produce a liquid if the temperature and pressure conditions are reduced further. A gas condensate on the other hand will form a two phase with

decreasing pressure, this happens on the dew point branch. The presence of heavy hydrocarbons expands the phase envelope relative to a wet gas. The reservoir temperature lies between the critical point and the cricondentherm. Gas condensate reservoirs are also referred to as a retrograde condensate reservoir because of the anomalous behavior it exhibits. A retrograde condensate is when a liquid is formed by an isothermal decrease in pressure or isobaric increase in temperature which is used to characterize these types of reservoir fluid. Both black and volatile oil will enter into a two phase at the bubble point line and the new phase formed will be gas if there is a substantial reduction in temperature and pressure. But the critical points differ in relative distance to the reservoir temperature condition which is shown by Fig 2.2 of the five types of reservoir fluid.

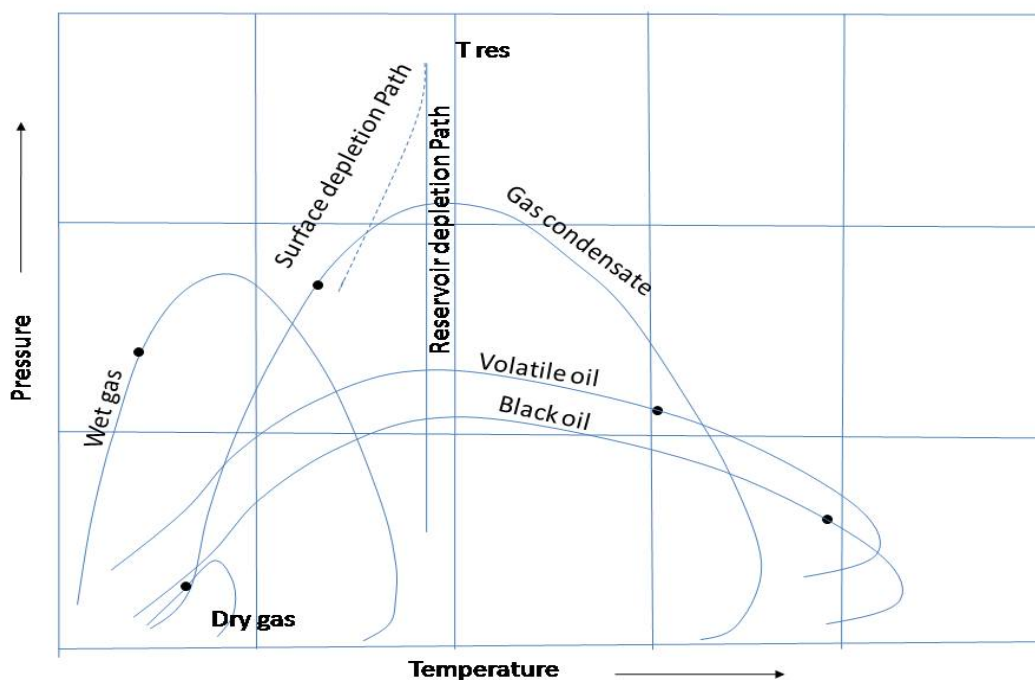


Figure 2-2: Phase envelope of the various types of reservoir fluids (after Pedersen and Christensen).

Nichita (2008) described the construction of a phase envelope as a very important problem in phase equilibrium calculation. This is due to its many applications in chemical thermodynamics and hydrocarbon reservoir thermodynamics. The different classes of the reservoir fluid are essential information for the proper design of petroleum processes. Phase envelopes are very useful in the design of surface facilities (e.g. separators), primary production, gas injection processes, enhanced oil recovery and design of pipeline networks for transportation of natural gas by pipeline or in liquefied natural gas (LNG). It is also a very good foundation for further studies of the complex nature of hydrocarbon reservoir fluids. It also has applications in ethane plus recovery, refrigeration processes and operation near critical point or supercritical region. The amount of experimental and theoretical work which has gone into the study of phase envelope construction indicates its importance in trying to solve the phase equilibrium problems faced by petroleum and refinery engineers in the petroleum industry and the general engineering field today.

## **2.1 Phase Envelope Calculations**

Phase equilibrium calculations started as far back as the late 1800's and the early 1900's with notable works by the likes of Gibbs and van der Waals who postulated the first equation of state in 1873. These two were among the first researchers to formulate the concepts and mathematical relationship in which a phase behavior of gases could be understood better. This relationship was very applicable to the petroleum industry which used traditional PVT correlations to analyze phase behavior of reservoir fluids.

In spite of the complexity of hydrocarbon fluids found in reservoir rocks, simple cubic equations of state have shown surprising performance in the phase behavior calculations for both the vapor-liquid and vapor-liquid-liquid equilibrium of these reservoir fluids. Equation of state is a thermodynamic equation which defines the state at which a given fluid or mixture is under given physical conditions, it also provides relationship between two or more state functions associated with the fluid. Peng-Robinson EOS and Soave RK EOS are the two most widely used equations of state in phase equilibrium calculations. Their equations provide simplicity and also a reasonable amount of accuracy for phase equilibrium calculations when compared with experimental data. Both equations of state were making modifications to the Van der Waal's earlier proposed equation. While SRK proposed a generalized empirical expression in terms of the acentric factor which provided a better vapor-liquid equilibrium results, Peng-Robinson's modifications made a slightly improved description of the liquid densities. However, Peng-Robinson's equation of state is more preferred in the oil and gas industry because it generates results which are in good agreement with experimental data for hydrocarbon mixtures.

### **2.1.1 Phase Envelope Construction**

There are various ways in which a phase envelope is constructed. Phase envelopes are essentially constructed by the determination of the bubble point and dew point line of a given system that are plotted on a PT diagram. This could be on a constant composition or constant temperature line. One method in which the points of a phase envelope could be obtained, is to determine them through experimental methods in a laboratory. A

simple laboratory test that could be used to determine the bubble point and dew point of multicomponent mixtures is through the use of PVT cells. These PVT cells could be operated at the value of pressure and temperature which are of interest. The PVT cells consist of a mechanism in which pressure and temperature can be varied. Pressure could be varied by either mercury injection\withdrawal or by a mechanically driven piston. Temperature can be varied with an instrument known as a climatic air bath. The saturation points are being noted visually. The noting of the vapor phase or liquid phase is done through a special window. Samples of a fixed composition are loaded from a separate chamber or are prepared directly in the PVT cell. Once a homogeneous single phase is achieved, pressure depletion is carried out by taking note of the phase changes through the window. This phase changes could also be monitored by video recording machine. The procedure is then repeated for a new isotherm. This method of determining the bubble points and dew points is both time consuming and expensive. The experimental method is not always the best way to achieve a phase envelope. In many cases it is not always possible to obtain laboratory measurements.

Another method for phase envelope construction is by using empirical correlations. Various empirical correlations have been generated from experimental results and field data which could also be used for estimating properties of reservoir fluids. Phase envelope could be constructed using correlations of the bubble points and dew points pressure. For bubble point pressure, some of the major correlations that are used are by Standing, Lasater, Vasquez-Beggs, Glaso and Maroun correlations. Standing (1947) developed the first accurate correlation which was from California oil. He proposed a

graphical correlation for determining the bubble point pressure and later expressed the graph by Eq. (2.1) shown below

$$P_b = 18.2[(R_s / \gamma_g)^{0.83}(10)^a - 1.41] \quad (2.1)$$

where:

$$a = 0.00091T - 0.0125(\text{API})$$

$P_b$  = bubble point pressure, psia

$R_s$  = solution gas to oil ratio SCF/STB

$T$  = Temperature, °F

Lasater (1953) used a different approach in which the mole fraction of solution gas was used as the main correlating parameter. In this approach the gas mole fraction is dependent mainly on solution gas/oil ratio. Lasater's correlation is given by equation Eq. (2.1) shown below

$$P_b = A \frac{T}{\gamma_g} \quad (2.2)$$

where the function  $A(y_g)$  interpolated graphically and can be described by,

$$A = 0.83918 \times 10^{1.17664y_g} y_g^{0.57246}; y_g \leq 0.6 \quad (2.2a)$$

$$A = 0.83918 \times 10^{1.08000y_g} y_g^{0.31109}; y_g > 0.6 \quad (2.2b)$$

$$y_g = \left[ 1 + \frac{133,000(\gamma / M)_0}{R_s} \right]^{-1} \quad (2.2c)$$

and,

$P_b$  = bubble point pressure, psia

$R_s$  = solution gas to oil ratio SCF/STB

$T$  = Temperature, °R

Glaso (1980) used Standing's approach for North Sea oils, where he made a correction for the non-hydrocarbon content and stock tank paraffinity which at the time was not widely used, due to the unavailability of data. His correlation is shown in by Eq. (2.1)

$$\log p_b = 1.7669 + 1.7447 \log A - 0.30218(\log A)^2 \quad (2.3)$$

where:

$$A = (R_s / \gamma_g)^{0.816} (T^{0.172} / \gamma_{API}^{0.989}) \quad (2.3a)$$

$P_b$  = bubble point pressure, psia

$R_s$  = solution gas to oil ratio SCF/STB

$T$  = Temperature, °F

There are fewer correlations for dew points compared to the bubble point. Amongst the few notable dew points correlations are the Nemeth and Kennedy (1967) in which a dew point pressure was proposed based on the composition of the  $C_{7+}$  and its properties. The Nemeth and Kennedy correlations is given by Eq. (2.1) shown below

$$\begin{aligned} \ln P_d = & \left[ Z_{c_2} + Z_{c_{O_2}} + Z_{H_2S} + Z_{c_6} + (Z_{c_3} + Z_{c_4}) + Z_{c_5} + 0.4Z_{c_1} + 0.2Z_{N_2} \right] + A_2 \gamma_{c_{7+}} \\ & + A_3 \left[ \frac{Z_{c_1}}{(Z_{c_{7+}} + 0.002)} \right] + A_4 T + (A_5 Z_{c_{7+}} M_{c_{7+}}) + A_6 (Z_{c_{7+}} M_{c_{7+}})^2 + A_7 (Z_{c_{7+}} M_{c_{7+}})^3 \quad (2.4) \\ & + A_8 \left[ \frac{M_{c_{7+}}}{(\gamma_{c_{7+}} + 0.0001)} \right] + A_9 \left[ \frac{M_{c_{7+}}}{(\gamma_{c_{7+}} + 0.0001)} \right]^2 + A_{10} \left[ \frac{M_{c_{7+}}}{(\gamma_{c_{7+}} + 0.0001)} \right]^3 + A_{11}, \end{aligned}$$

where:

$A_1 = -2.0623054$ ,  $A_2 = 6.6259728$ ,  $A_3 = -4.4670559 \times 10^{-3}$ ,  $A_4 = 1.0448346 \times 10^{-4}$ ,  $A_5 = 3.2673714 \times 10^{-2}$ ,  $A_6 = -3.6453277 \times 10^{-3}$ ,  $A_7 = 7.4299951 \times 10^{-5}$ ,  $A_8 = -1.1381195 \times 10^{-1}$ ,  $A_9 = 6.2476497 \times 10^{-4}$ ,  $A_{10} = -1.0716866 \times 10^{-6}$  and  $A_{11} = 1.0746622 \times 10^1$ .

This correlation is applicable to dew points pressure between 1,000 and 10,000 psia and temperatures from 40 to 320°F with a wide range of reservoir compositions. The accuracy of the dew points pressure is between +/- 10%. This is because the experimental accuracy is determined with only +/- 5%. Other correlations used for dew points pressure are Organick and Golding (1952) and Kurata and Katz (1942), both of which were presented in graphical forms.

Empirical correlations are developed for specific petroleum reservoir fluids originating from a specific geographical field. The correlations typically match the employed experimental data with a reasonable error percentage. Due to the peculiarity of empirical correlations, many of them have limited applicability and can produce large errors when applied to reservoir fluid samples from other geographical fields. These correlations all have various limitations in which their applications are successful.

Equation of state has found reasonable success in phase envelope and phase equilibrium calculations. Asselineau, Bogdanic and Vidal (1979) proposed an algorithm for the construction of a phase envelope in which they paid special attention to the applicability of the method in critical and high-pressure regions because of the trivial solutions which was attained with false unit of equilibrium constants. Their procedure was said to be

applicable to any analytical equation of state. Their method involves the simultaneous solution of  $2n+4$  equations for each point of the phase envelope (where  $n$  is the number of components in the system). The method proposed gives an initial guess of the unknowns and ensures a successful iterative procedure. The derivative used was obtained as soon as equilibrium was attained since the Newton-Raphson is highly sensitive to the initial guess. This was made to diagnose the retrograde condensation process and provides a rapid stepwise calculation. Michelsen's (1980) proposition, which was later corroborated by Yau-Kun and Long (1982) in their review of phase envelope construction to be a very efficient algorithm for the phase envelope point's calculations. Michelsen formulated the simultaneous solution of  $n+2$  equations for each point calculations rather than the single solution of two simultaneous non linear equations as earlier proposed by Asselineau et al. In order to enhance the convergence, this algorithm selects internally the set of primary variables and the step size to the subsequent point on the diagram. The initial guess is obtained by extrapolation. He also suggests that Newton-Raphson scheme should be used in the critical region and the retrograde regions as a solution for the non-linear equations. With this, an automatic selection of the better convenient specification variable is obtained from the previous calculation for the saturation points. Yau-Kun and Nghiem (1982) developed a general phase envelope algorithm which was an extension of the work by Michelsen, in which the bubble point and dew point are traced in one pass. The method was extended to the generation of phase envelopes on pressure-composition, temperature-composition and composition-composition diagrams. Yau-Kun et al. (1982) highlighted the major difficulties which are associated with phase envelope generations as:

1. Tracing the dew point line is a tedious task. This is because of the presence of a lower dew point and upper dew point of mixtures.
2. Near the critical region it is not clear which of the saturation line is to be iterated i.e. whether it is the bubble point or the dew point line.
3. Also that the variable specification is done manually for example while constructing a pressure-temperature diagram in terms of the pressure and temperature values.

Ziervogel and Poling (1983) made another attempt to improve on the method of calculation of phase envelopes points for multicomponent mixtures. In their work they proposed a simple method in which an initial guess was to be iterated while drawing the bubble point line and another guess for the dew point line. This method is easier than previous methods because the bubble point and dew point are determined by iterating on a single variable through the critical region. Their work used Soave's modification of the Redlich-Kwong equation of state, which was used in the phase envelope point's calculation by Michelsen (1980) and Asselineau et al (1979). They used the same method of calculating the dew and bubble points, which is by stepping around the phase envelope in small increments of pressure or temperature values. To generate the complete phase envelope the bubble points are first calculated. The calculation is started at low pressure up-to the critical point, after this the dew point curve is then generated. Their method's success is primarily guessing on which iteration variable is to be used during either the dew point or the bubble point calculation. The method works because derivatives with

respect to only one variable are needed for convergence. And this depends on the success of selecting the right variable as the iteration parameter. When comparing the complexity of the calculations, it is an improvement to the earlier proposed methods. Although the emphases on the iteration method being correct for calculation of phase envelopes in choosing the iteration parameter was not tested for all cases of reservoir fluids. Also near the critical region, it is not clear whether a bubble point or dew point should be computed and the specifications of the variables to be iterated are done manually.

Michelsen (1994) later used a method in which the phase envelope was to be calculated without the iterative determination of equilibrium phase compositions. The individual points on the phase envelopes were solved by using two equations, irrespective of the number of the components in the mixture. The requirement for the composition derivatives of the fugacity coefficient was developed. His method is not based on a full Newton-Raphson procedure. The method is said to be simple because the rate of the convergence is not adversely affected in the critical region. One of the limitations of this method is that the solution at a given temperature and pressure cannot be obtained directly. Instead, it should be calculated or interpolated.

Firoozabadi (2003) compared various calculations steps in characterizing the non linear equations which define the two phase flash calculations. The methods investigated were the successive substitution method, the Newton's method, the dominant eigenvalue method and the global convergent Newton method. This work suggested the tangent plane distance for the equilibrium calculation's initialization. Either the Newton's method

or the successive substitution method combined with the tangent plane distance can greatly make the two phase calculations relatively easier according to the authors. But what was not investigated was how efficient the suggested algorithm was, compared to other algorithm for the two phase flash calculation for phase envelope points. Nitichita (2007) recently used a reduction method for phase equilibrium calculations in his work. In the method he replaced the traditional variables such as mole numbers, mole fractions, partition coefficient with some linear combinations of them. He took advantage of the Jacobian matrix extrapolation from the previous step calculations. This work had the robustness and efficiency for larger number natural hydrocarbons with as many as 24 components.

Another class of equation which could be used to calculate phase envelope points is known as the non cubic equation of state. Alfradique (2007) compared the performance of the one cubic equation to two other non cubic equations. In his work he stated that the most widely accepted of the non cubic equation of states are the SAFT family and the modifications like PC-SAFT and SAFT-VR. It was noted that the non cubic equation of states error margin was much greater than the conventional cubic equation of state like Peng-Robinson EOS comparing it with at least 29 multicomponent hydrocarbon mixtures.

## **2.2 Critical, Cricondenbar and Cricondenthem Calculations.**

Three distinct points define the shape and location of a phase envelope. These three points are known as the critical point, cricondenbar and cricondenthem as illustrated in Fig 2-2. The cricondenthem is defined as the highest temperature at which a mixture can exist in both liquid and vapor phase together, while the cricondenbar is the highest pressure at which a mixture can exist in the two phase regions. For a gas condensate reservoir the cricondenthem and cricondenbar are important from production, transportation and processing viewpoints. Lastly, the critical point is the point at which there is no distinct difference between the vapor and liquid phase. At this point, the two phases become indistinguishable. The critical point could also be defined as the point at which the dew point line and the bubble point line meets. This critical point defines a unique state for vapor and liquid coexistence in a reservoir fluid. All three points can be determined experimentally. The cricondenthem and cricondenbar can both be extrapolated from a complete phase envelope construction but the critical point has to be determined either experimentally or through calculations which utilize either correlations or equations of state equilibrium flash algorithm.

Due to the sensitivity related to the point for single and multicomponent hydrocarbons, there have been several methods used for calculating the critical points of natural gas mixtures.

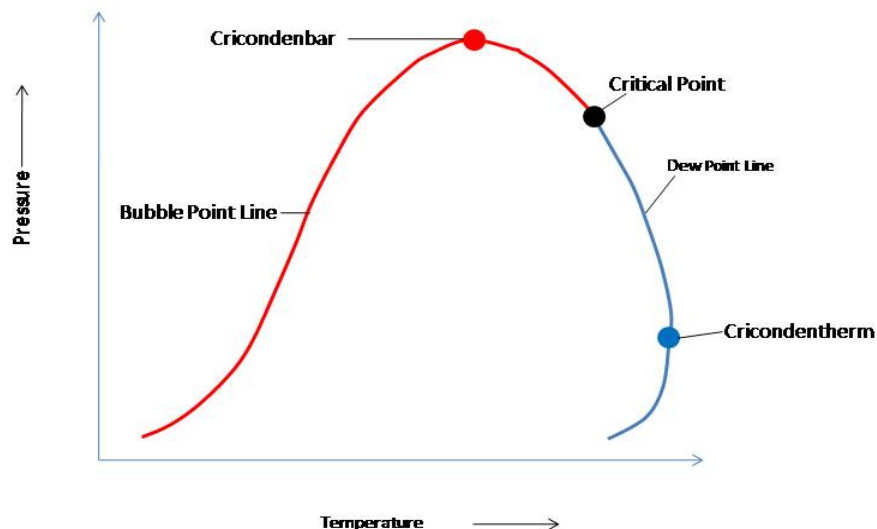


Figure 2-3: Phase envelope showing cricondentherm, cricondenbar and critical point.

Attempts have been made at calculating the cricondentherm and cricondenbar of hydrocarbon fluid. Etter (1961) came up with an empirical correlation for the calculation of critical, cricondentherm and cricondenbar's pressure and temperature value of phase envelope for multicomponent mixtures of normal paraffins i.e. of hydrocarbon with relatively low molecular weight and light hydrocarbons. A set of equations to calculate the pressure and temperature value of the critical, cricondentherm and cricondenbar were generated from plotting the critical pressure and the average molecular weight and also from a plot of the temperature with the average molecular weight for binary mixtures. The reason for this limitation to the empirical equation proposed was that most of the

data available at this time were for these classes of hydrocarbon. Hence, the critical properties could be calculated with the equations below for the temperature and pressure:

$$(P_c)_{mix} = \sum x_i P_{c_i} + \sum \Phi(P_{ctd_i}, x_i) \quad (2.5)$$

$$(T_c)_{mix} = \sum W_i T_{c_i} + \sum (T_{c_{xi}} - T_{c_{x=0}}) \quad (2.6)$$

for cricondentherm the pressure and temperature is given by:

$$(P_{ct})_{mix} = \sum x_i P_{c_i} + \sum (P_{ctd_i}, x_i) \quad (2.7)$$

$$(T_{ct})_{mix} = \sum W_i T_{c_i} + (T_{ctd})_{xL} \sum (T_{ctd}) \quad (2.8)$$

and cricondenbar pressure and temperature is calculated with:

$$(P_{cb})_{mix} = \sum x_i P_{c_i} + \sum \Phi(P_{ctd_i}) \quad (2.9)$$

For  $\Phi \sum W_{ci} < 0.5$ ,

$$(T_{cb})_{mix} = \sum W_i T_{c_i} + \sum (T_{cb_{ci}} - T_{cb_{i-1}}) \quad (2.10)$$

While  $\sum W_{ci} > 0.5$ ,

$$(T_{cb})_{mix} = \sum W_i T_{c_i} + \sum (T_{cbd})_i \quad (2.11)$$

where

x = mole fraction,

$\Phi$  = function of,

W = weight fraction,

L = lighter component,

i = any component.

P and T denote pressure (psia) and temperature ( $^{\circ}$ R) respectively. The subscript c, ct and cb represent critical, cricondenthem and cricondenbar respectively. While the subscript cd, ctd and cbd represent the excess critical, excess cricondenthem and excess cricondenbar.

The excess pressure and temperature is the critical temperature and pressure calculated as the product sum of the critical constant and the compositions of all the components, in which the lowest molecular weight component produces the greatest effect in proportion to the amount present. These empirical calculations are specific to individual paraffin which requires constants which are not easily obtainable. Although it was shown that this method gives reasonable result with the normal paraffin investigated, Thodos and Silverman (1962) came up with an equation to solve for the temperature and pressure value of cricondenbar and cricondenthem. They used statistical techniques to develop a relationship between the characteristics of binary hydrocarbon and the temperature and pressure of the two points on the phase envelope. The equation formulated was highly inaccurate for methane systems Grieves and Thodos (1963). Grieves et al (1963) gave a similar correlation for calculating the cricondenthem and the cricondenbar temperature. He developed a correlation using graphical interpretation. His work was more general for reservoir fluid with higher error percentage, which was as high as 2.41 and low as 0.26 for cricondenthem and was in the range of 0.12-4.27% for the cricondenbar temperature when compared with experimental data. To calculate the temperature for the cricondenthem and cricondenbar the information needed was the critical temperatures of the pure components, normal boiling points and approximate vapor pressures. For the

calculation of the temperature of the cricondenthem and cricondenbar he gave the equations below:

$$T_t / T_c - 1 = \left( \frac{T'_b}{T_b} - 1 \right) \left( e^{5.40x\ell - 3.39} \right) + 0.01; 0 < x\ell \leq 0.55 \quad (2.12)$$

$$T_t / T_c - 1 = \left( \frac{T'_b}{T_b} - 1 \right) \left( e^{6.38x\ell - 4.38} \right) - 0.418x\ell + 0.256; 0.55 < x\ell < 0.925 \quad (2.13)$$

$$T_p / T_c - 1 = \left( \frac{T'_b}{T_b} - 1 \right) \left( e^{4.33x\ell - 3.62} \right) + 0.008; 0 < x\ell < 0.7 \quad (2.14)$$

$$T_p / T_c - 1 = \left( \frac{T'_b}{T_b} - 1 \right) \left( e^{6.33x\ell - 5.14} \right) - 0.165x\ell + 0.116; 0.7 < x\ell \leq 0.925 \quad (2.15)$$

where,

$T_t$  = cricondenthem temperature, °R

$T_p$  = cricondenbar temperature, °R

$T_b$  = atmospheric boiling point of mixture, °R

$T'_b$  = normal boiling point of  $i^{\text{th}}$  component, °R

$T'_c$  = pseudocritical, pseudocricondenthem, or pseudocricondenbar temperature of mixture (method of calculation depends on number of components), °R

$x\ell$  = mole fraction of low-boiling component.

Grieves et al (1963) in a follow up work, made the same empirical correlations for the cricondenbar and cricondenthem pressures. Comparing with experimental data they had an error percentage as high as 13.98 and low as 0.88 for cricondenthem pressure. While for the cricondenbar pressure they had percentage errors from the range of 0.84-9.52. The

pressure values were more directly related to the plot of  $P_t / P_{pc}$  versus  $T'_b / T_b$ . Which the cricondenthem pressure can be directly solved from. Also the cricondenbar pressure was extrapolated from the plot of  $P_p / P_{pc}$  versus  $T'_b / T_b$ .

Where:

$P_p$  = cricondenbar pressure of mixture, psia

$P_t$  = cricondenthem pressure of mixture, psia

$P_{pc}$  = pseudocritical, pseudocricondenthem, or pseudocricondenbar pressure of mixture (method of calculation depends on number of components), psia

Taraf, Behbahani and Moshfeghian (2008) generated a numerical algorithm for the direct calculation of the cricondenthem and cricondenbar pressure and temperature of natural gas of known composition which he based on Michelsen's (1985) method. This method was based on the fact that the derivatives of the pressure with respect to the temperature at the cricondenbar are equal to zero and also the derivatives of the temperature with respect to pressure at the cricondenthem are equal to zero. Their method also utilizes the equality of fugacity for each component in both phases. They proposed that for the cricondenthem and cricondenbar calculation should be done by:

- First make an initial guess for temperature and pressure
- Calculate initial liquid mole fractions ( $x_i$ ), n using Eq. (2.16) to solve simultaneously with initial guesses of temperature and pressure

$$g_n = \ln(z_i) - \ln(x_i) + \ln(\Phi_i^v) - \ln(\Phi_i^l) = 0 \quad (2.16)$$

where:

$z_i$  = mole fraction of component in mixture

$x_i$  = component liquid phase mole fraction

$\Phi_i^v$  = fugacity coefficient of component  $i$  in vapor phase

$\Phi_i^l$  = fugacity coefficient of component  $i$  in liquid phase

$Q$  = modified tangent plane distance

- With the values of  $x_i$  and temperature solve for  $dQ/dT=0$  for a new temperature for cricondenbar or  $dQ/dP$  for a new pressure for cricondentherm.
- Perform Newton's iteration using Eq. (2.16) and Eq. (2.17) with the new pressure/temperature which was earlier calculated in the previous step

$$g_{n+1} = 1 - \sum_1^n x_i = 0 \quad (2.17)$$

- If the temperature/pressure does not converge go back to the third step.

They also investigated the ranges for the initial guesses. This was said to be of a value in the two phase region. The proposed algorithm was found to be in excellent agreement with experimental results and values from common simulation software for the cases tested.

For the critical point calculations various methods have been proposed for the direct calculation. Due to the peculiarity of the critical point of multicomponent mixtures,

Firoozabadi (2006) explained that the composition changes which occur is so often in some applications that there is a need to calculate the critical point as many as  $10^8$  times. A major motivation of their work was that current method's lack robustness and efficiency for the calculation of the critical point for multicomponent mixtures. Most of the current methods were based on decreasing the pressure in some increments and carrying out phase split calculations. These methods mostly require rigorous calculations with as much iteration, which are very time consuming and predictions are not 100% accurate because of errors associated with equilibrium calculations.

A major correlation can be derived from the cricondentherm, cricondenbar and the critical point of a phase envelope with the composition of a reservoir fluid. If such a relationship can be established, it will capture and represent the equilibrium calculations for phase envelope construction which is associated with the complex nature of natural gas reservoirs. The principal challenge if this research therefore, is to try and establish the most effective neural network that can give the best results in making these predictions in terms of the temperature and pressure values; and to also determine which of the input parameter is most relevant in this relationship. It will be of paramount interest to be able to estimate the critical points, the cricondentherm (highest temperature) and the cricondenbar (highest pressure) through the help of an expert system. In doing this, a faster and more convenient way of constructing the phase envelope through the temperature and pressure of the key points will be presented.

The importance of phase envelope to the petroleum industry cannot be over emphasized. The accuracy of being able to predict the location of the critical temperature and pressure

along with the cricondenthem and cricondenbar goes a long way in being able to get a better phase envelope and enhance our understanding of the fluid/gas in the reservoir. Artificial neural network (ANN) would eliminate the time for extensive phase equilibrium calculations needed for the prediction of the phase envelope through the generation of an expert system. This expert system is intended to understand the non linear relationship between various natural gas reservoir compositions of  $C_1$ - $C_{7+}$ , specific gravity and the molecular weight of the  $C_{7+}$  with the critical points, the cricondenthem and cricondenbar pressure and temperature values for faster estimation of the shape of the phase envelope.

### **2.3 Artificial Neural Network**

The complexity of how information is being analyzed by the brain has been the focus of research for the past decade. It has been known that the human brain utilizes  $10^{11}$  neurons (biological) while trying to understand and facilitate reading, breathing, motion and thinking. Each of these biological neurons is a rich assembly of tissues that has the complexity, if not the speed, of a microprocessor. Part of this was formed at birth while the others were formed by experience. In the quest for better and faster solutions to the very complex engineering problems, the artificial neural network (ANN) was formed. This neural network was aimed at trying to mimic the behavior of the biological neurons Fausett (1994).

Neural network has been described as a network of simple processing elements (neurons), which can exhibit complex global behavior, determined by the connections between the processing elements and the element parameters. The efficiency of the

artificial neural network can still not be compared with the biological neural but still, similarities exist that cannot be denied in their mode of achieving the task. These similarities are:

1. The building blocks of both networks are through simple computational devices which are extremely interconnected.
2. Also, the connections between them determine how efficient the network is.

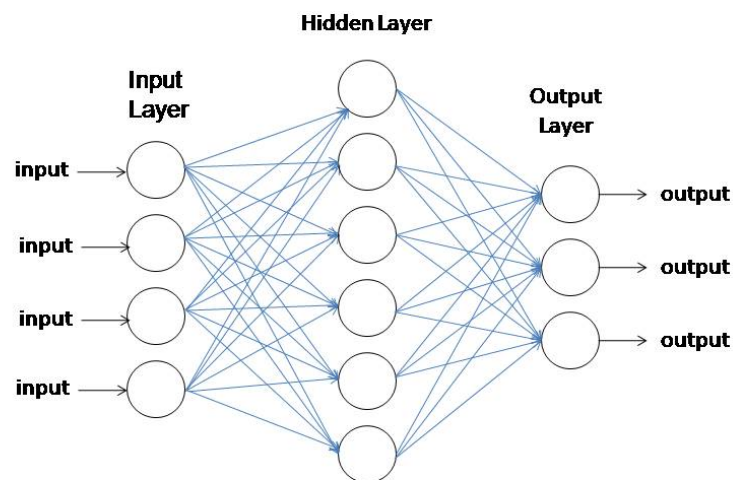


Figure 2-4: Neural network with three layers

A typical example of an interconnected neural network architect is shown in Fig 2-4 where the network utilizes a three layer system with four inputs and three outputs that are arranged in multiple layers. Every neural network possesses knowledge which is contained in the values of the connections weights. Stergiou C and Siganos D (2007)

explained that changing the knowledge stored in the network as a function of experience implies a learning rule for changing the values of the associated weights. For example each input parameter in Fig 2-4 has its own weight with it. Demuth and Beale (2003) stated that there are essentially two types of training which is utilized in training a neural network. These are known as the supervised and the unsupervised training. The supervised training applies an external boundary, so that each output unit is told what its desired response to input signals ought to be. During the learning process global information may be required. Examples of supervised learning include error-correction learning, reinforcement learning and stochastic learning. An important issue concerning supervised learning is the problem of error convergence, i.e. the minimization of error between the desired and computed unit values. The aim is to determine a set of weights which gives the least error. One well-known method, which is commonly used in many learning paradigms, is the least mean square (LMS) convergence. But the unsupervised learning uses no external boundary and is based upon only local information. This is also known as self-organization, in the sense that it re-organizes data presented to the network and detects their developing collective properties. An example of unsupervised learning is competitive learning. From human neurons to artificial neurons other aspect of learning concerns the distinction or otherwise of a separate phase, during which the network is trained, and a following operation phase. A neural network is said to learn off-line if the learning phase and the operation phase are distinct. A neural network learns on-line if it learns and operates at the same time. Usually, supervised learning is performed off-line, whereas unsupervised learning is performed on-line.

The performance of a neural network basically depends on the weight and the transfer functions (which are the input and output functions). These functions are basically categorized into three groups, namely: the sigmoid, linear and threshold. For the sigmoid the output varies continuously but not linearly as the input changes. Sigmoid units bear a greater resemblance to real neurons than do linear or threshold units, but all three must be considered rough approximations. In the linear transfer function, the output activity is proportional to the total weighted output. While for the threshold transfer function the output is set at one of two levels, depending on whether the total input is greater than or less than some threshold value (Neural Network Toolbox).

Hagan, Demuth and Beale (1996) gave the general order to train a neural network to perform some task, in which the weights must be adjusted. This adjustment is such that the error between the desired output and the actual output is reduced. This process requires that the neural network compute the error derivative of the weights (EW). In other words, it must calculate how the error changes as each weight is increased or decreased slightly. The back propagation algorithm is the most widely used method for determining the error derivative of the weights.

### **2.3.1 Backpropagation Learning**

Backpropagation is said to be the simplest neural networks algorithm in which the information flow is in one path (Neural Network Toolbox). This is an example of supervised learning in which an input vector and the corresponding output (target) vector are used to train the network until it can approximate a function, associate input vectors

with specific output vectors, or define input vectors in an appropriate way as defined in the training algorithm. In a more complex problem, information can flow in more than one direction. Conjugate gradient backpropagation uses `traincgf` as a network training function. The `traincgf` updates weight and bias values according to conjugate gradient backpropagation. The backpropagation learning type of learning algorithm was used in this work. Training stops when either one of the following stipulated condition is met. The conditions are either:

- The specified maximum number of epochs (repetitions) is reached
- The maximum amount of time is exceeded( if specified)
- The performance is minimized to the goal.
- The total number of iterations is reached.

The artificial neural network finds its uses in a variety of industries such as medicine, banking and finance, marketing, and also in the petroleum industry. Extensive research has been done on how applicable ANN is, especially to the oil and gas industry. In drilling engineering, artificial neural network as been useful to solve for optimum bit selection Yilmaz, Demircioglu and Akin (2002) and applied to predicting the operating conditions for optimum surface condensate recovery that yields the highest API gravity an aspect of petroleum production engineering Al-Farhan and Ayala (2006), furthermore in reservoir studies to understand the compositional behavior of gas cycling operations in gas condensate reservoirs Ayala and Ertekin (2007). ANN proves to be a powerful and viable tool in our industry today with further research being undertaken daily.

Mann (2007) used artificial neural network to generate an intelligent system for the design of natural gas storage facility. In his study, he utilized artificial neural network in two ways. First he used it to model the behavior of a gas storage facility, secondly he then used ANN for actual design optimization of a storage facility. He proposed a network of ten input neurons and four output neurons connected by two hidden layers. These two hidden layers had fifty and twenty five neurons respectively.

Briones et al (1994) also found ANN to be applicable in the prediction of reservoir hydrocarbon mixture composition using production data. They used input parameters such as the GOR and API of two Venezuelan regions with marked differences in the fluid properties. With their target (output parameter) being the composition of  $C_1$ ,  $C_2-C_6$ ,  $C_{7+}$  and  $CO_2$ . Their network showed another applicability of how useful ANN is in the petroleum industry. With being able to predict accurately a system of fluid composition based on earlier production parameters.

In utilizing ANN for equilibrium conditions predictions, Gonzalez, Barrufet and Startzman (2003) proposed an expert system to predict dewpoint pressure of retrograde gases which they achieved with an average error of 8.74% which is more reliable than the multiple regression techniques. Using an experimental data of the dew point pressure to train the network they were able to achieve their goal with one input layer with 13 neurons and one hidden layer with 6 neurons and one output layer with one neuron. In comparing their results with the available correlations it was found that neural network is much more in agreement with the experimental data than the equations of state which is

the best empirical correlation in estimating phase equilibrium. Birang et al (2007) also used neural network model to predict the minimum miscibility pressure for hydro carbon gas injection processes, in which both the condensing and vaporizing mechanism of the gas flooding was going to be considered to produce a robust model which will be applicable to any composition no matter which mechanism is dominant in achieving miscibility. Moghadassi, Parvizian and Hosseini (2009) from experimental data, training with back propagation used a new method which was based on artificial neural network to solve for vapor-liquid equilibrium data for a binary system (nitrogen-n-pentane) for improving oil recovery for nitrogen injection into reservoirs.

To estimate the pressure and temperature values for the construction of a phase envelope, neuro simulation study is carried out. ANN seems very plausible for training an expert system that would achieve these goals. Using FOTRAN© for the thermodynamic calculations coupled with soft computing tool MATLAB®. The network will understand the relationship between the input parameter (natural gas compositions and properties) and the output parameter (pressure and temperature corresponding to the critical point, cricondentherm and cricondenbar) for this prediction to be possible. The expert system ANN should be able to predict this temperature and pressure values which would be used to predict the relative shape and position of a phase envelope.

## **Chapter 3**

### **Problem Statement**

A proper analysis of many petroleum problems requires knowledge of at least a portion of the phase diagram. An accurate knowledge of natural gas phase behavior is of essential value for both industrial processes and optimum operating conditions. Calculation method for phase envelope points is classified into two main types. These are the equilibrium flash calculations and the Gibbs energy minimizations. These points could also be experimentally determined.

Three points can be used to define the characteristics and shape on the phase envelope of natural gas. These points are known as critical point, the cricondetherm and the cricondenbar. If these three points can be predicted with good accuracy the entire phase envelope can be well approximated. Great importance is then attached to the cricondetherm, cricondenbar and the point of criticality of pressure and temperature values. These three points on the phase envelope will in great essence help in estimating the shape of a phase diagram of a reservoir fluid or gas which shows the region which the liquid and vapor will coexist.

In the past, general empirical correlations and relationships have been proposed for the cricondetherm, cricondenbar and the critical point. This work considers the three points which defines the phase envelope to be estimated with relations to just the compositions

of natural gas, specific gravity of  $C_{7+}$ , with the molecular weight of the  $C_{7+}$  as the input parameter. This research work with the aid of a neural network aims to help in point's calculation which is particular to phase envelope construction. It also aims at giving a faster and reliable pressure and temperature values for the phase envelope estimation for a robust range of natural gas composition.

This study presents an expert system that utilized the advantages of ANN in which speed, simplicity is used to learn the relationship between the input parameters (compositions of methane  $C_1$ , ethane  $C_2$ , propane  $C_3$ , butane  $C_4$ , pentane  $C_5$ , hexane  $C_6$ , heptanes  $C_{7+}$ , hydrogen sulfide  $H_2S$ , nitrogen  $N_2$ , and carbon dioxide  $CO_2$  and also molecular weight of the  $C_{7+}$  (MW  $C_{7+}$ ) with the specific gravity of  $C_{7+}$  (SG  $C_{7+}$ )) and the output parameters (corresponding pressure and temperature value of critical, cricondenthem and cricondenbar). The model will also be able to analyze which of the input parameter is most relevant in relation to the corresponding output for the critical point, cricondenbar, cricondenthem pressure and temperature. Lastly, the network proposed will enable us to find the most relevant of the input to influence the entire phase envelope model (combining all three points pressure and temperature value).

## Chapter 4

### ANN Model Development

The state/phase in which a natural gas mixture exists is greatly sensitive to temperature and pressure conditions. Different factors account for these pressure and temperature condition in which this multicomponent mixture of hydrocarbons exists as. This sensitivity can be captured by a phase diagram which consists of an envelope. The phase envelope shows the most complete, straightforward and visual representation of the behavior of the fluid in different phases with the corresponding temperature and pressure ranges. For this reason an improvement in the construction of the phase envelope is being focused on using the artificial neural network.

This neural network utilizes the characteristics related to each natural gas composition's phase envelope. These characteristics include the composition of the natural gas mixture (H<sub>2</sub>S, CO<sub>2</sub>, N<sub>2</sub>, C<sub>1</sub>, C<sub>2</sub>, C<sub>3</sub>, C<sub>4</sub>, C<sub>5</sub>, C<sub>6</sub>, C<sub>7+</sub>.) as well as the specific gravity and the molecular weight of the C<sub>7+</sub>. Characterization of the C<sub>7+</sub> is an important aspect of the pressure-volume-temperature (PVT) predictions and phase envelope calculations.

1840 different mixtures were generated for this work. Great deal of importance is placed on the data which is being used to train and establish the nonlinear relationship between the input and output variables. Thorough and careful selection process was utilized in the creation of the data set which was used to train the neural network for the phase envelope.

The data were generated through the use of FORTRAN compiler. A program was written to generate different natural gas composition combination. So as to have wide range of

data set to train the network with. Hydrocarbons compositions used are methane  $C_1$ , ethane  $C_2$ , propane  $C_3$ , butane  $C_4$ , pentane  $C_5$ , hexane  $C_6$ , and heptanes  $C_{7+}$ . With non hydrocarbon present as hydrogen sulfide  $H_2S$ , nitrogen  $N_2$ , and carbon dioxide  $CO_2$ . Lastly, the molecular weight of the  $C_{7+}$  (MW  $C_{7+}$ ) and specific gravity of  $C_{7+}$  (SG  $C_{7+}$ ) accounting for the  $C_{7+}$  hydrocarbons. The sum of all the composition of in the mixture must be equal to 1. Hence the equation total mixture composition is given as Eq. (4.1)

$$\Sigma (\text{Total Component in the Mixture compositions}) = 1 \quad (4.1)$$

To make sure that there was a good distinction of the data created. A plot showing the variation of the input data set used comparing the networks training and testing. As shown for  $C_1$  in Fig 4-1. This aimed at making sure that an even distribution of the natural gas compositions was created for the phase envelope points for both the training and the testing of the neural network model.  $C_1$  composition was generated using Eq. 4.2 given below and bounded by Eq. 4.1 for all the possible combination of natural gas mixture which had a  $C_1$  composition of value greater than 0.403 or as specified.

$$C_1 = 1 - [\Sigma(CO_2 + N_2 + H_2S + C_2 + C_3 + C_4 + C_5 + C_6 + C_{7+})] \quad (4.2)$$

The data selected for the artificial neural network was carefully selected to generate a have a wide range of the phase envelope point's pressure and temperature values for the network proposed. The possible natural gas combination with the ranges of inputs data given in Table 4-1 would obviously be infinite. The total mixture composition that was selected for the study was a true representative range of composition that would give the

largest pressure and temperature values of the cricondenthem, cricondenbar and the critical point from the entire data that was generated.

The range of the input data that was generated is shown in Table 4-1 where the minimum and maximum values of the input data are highlighted. Table 4-2 displays the intermediate values utilized during the creation of the data set.

Table 4-1: Phase envelope input data range

Inputs	Minimum	Maximum
Hydrogen Sulfide, H <sub>2</sub> S	0.0000	0.1500
Nitrogen, N <sub>2</sub>	0.0000	0.1500
Carbondioxide, CO <sub>2</sub>	0.0000	0.1500
Methane, C <sub>1</sub>	0.4030	0.9400
Ethane, C <sub>2</sub>	0.0100	0.2000
Propane, C <sub>3</sub>	0.0040	0.1300
Butane, C <sub>4</sub>	0.0050	0.1200
Pentane, C <sub>5</sub>	0.0050	0.1200
Hexane, C <sub>6</sub>	0.0050	0.1200
Hepatane-Plus, C <sub>7+</sub>	0.0100	0.2000
Molecular Weight MW C <sub>7+</sub> ( lb/lbmol)	100	260
Specific Gravity, SG C <sub>7+</sub>	0.6000	0.8800

Table 4-2: Phase envelope possible actual values used for training

	Min	Max	Units	Examples of values used for training
H <sub>2</sub> S	0	0.15	fraction	0.00,0.01,0.02,0.05,0.037,0.15,0.112
N <sub>2</sub>	0	0.15	fraction	0.00,0.01,0.02,0.05,0.037,0.15,0.112
CO <sub>2</sub>	0	0.15	fraction	0.00,0.01,0.02,0.05,0.037,0.15,0.112
C <sub>1</sub>	0.404	0.94	fraction	0.404,0.454,0.51,0.62,0.74,0.83,0.94
C <sub>2</sub>	0.01	0.2	fraction	0.055,0.15,0.01,0.02,0.067,0.03,
C <sub>3</sub>	0.004	0.13	fraction	0.01,0.03,0.045,0.01,0.13,0.04,0.004
C <sub>4</sub>	0.005	0.12	fraction	0.033,0.093,0.01,0.05,0.08,0.12
C <sub>5</sub>	0.005	0.12	fraction	0.05,0.1,0.055,0.04,0.033,0.08,0.093
C <sub>6</sub>	0.01	0.1	fraction	0.04,0.03,0.085,0.053,0.01,0.066
C <sub>7+</sub>	0.01	0.16	fraction	0.126,0.01,0.053,0.085,0.03,0.16
MW C <sub>7+</sub>	100	260	lb/lbmol	100,120,160, 180, 200, 220, 240,260
SG C <sub>7+</sub>	0.6	0.88	unitless	0.6,0.63,0.67,0.74,0.79,0.81,0.88

Fig 4-1 displays the frequency of  $C_1$  – data employed for the creation of the testing and training data set. This histogram shows the frequency of methane composition in the natural gas mixture used for training and testing of the networks. The figure shows that the variation of the methane ( $C_1$ ) which was used in the network training and testing data was larger for natural gas composition within the range of 0.45-0.55 methane.

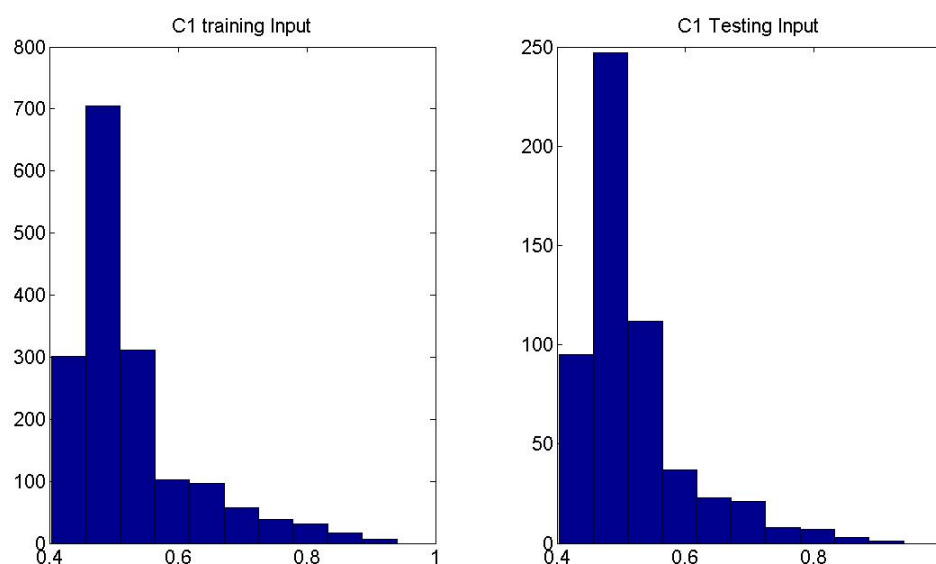


Figure 4-1:  $C_1$  Ranges for Training and Testing

#### 4.1 Phase Envelope Neural Network Data

One of the most important factors in training an efficient neural network model is to choose the content and source of the data which will be used for training and testing the neural network carefully and accurately. This is why various methods in which we could acquire data were investigated and carefully screened.

In order to generate the data needed for the network a phase envelope algorithm had to be used. The algorithm which was used to generate the data for the phase envelope points is based on Gibbs tangent plane criterion, which establishes the thermodynamic stability of a phase. This method of phase calculation known as the Michelsen's Stability or the tangent plane method. Michelsen (1982) proposed this method which initial estimates for the number of phases present at equilibrium or either for the equilibrium factors is not specified at the beginning of the calculation. The method finds whether a given composition has a lower energy remaining as a single phase which is also the stable phase or whether the mixture Gibbs energy will reduce by splitting the mixture into two or more phase which is the unstable region. Phase stability is whether a mixture at a given temperature and pressure can attain a lower energy by splitting into two or more phases. The Gibbs energy for a composition  $z_i$  is given as Eq. (4.1)

$$G_z = \sum_{i=1}^N (n_i \mu_i)_z \quad (4.1)$$

And if the mixture will split into two phase then  $G_z$  is greater than  $G_{mix}$  where  $G_{mix}$  is given as Eq. (4.2)

$$G_{mix} = \sum_{i=1}^N (n_i \mu_i)_V + (n_i \mu_i)_L \quad (4.2)$$

where:

$G_{mix}$  = Gibb's energy of mixture

$n_i$  = no of components

$\mu_i$  = chemical potential of component i within a phase

The phase stability or the “Michelsen’s Stability” test allows us to predict the number of phases of the fluid. The phase stability comprises of formation of two hypothetical vapor and liquid like phases using the overall composition data provided. This data (phase stability) when combined with the entire algorithm helps to predict the fluid behavior at a higher level of intricacy thus increasing its precision. The tangent plane distance uses a tangent to the Gibbs minimum energy curve (which is plotted assuming a single phase exists) at the overall composition of the mixture (which is being tested for stability) for a particular temperature and pressure. Then a trial phase is created such that the tangent to the Gibbs minimum energy curve is parallel to the tangent drawn before. Now if the new tangent lies below the previous one then the mixture being tested then it is unstable and the phase split will occur otherwise single phase is stable. For our case single phase stability is tested only against two phase to obtain a phase envelope representing vapor liquid equilibrium. And once two phases is achieved a phase envelope data is extracted for the mixture which corresponds to the temperature and pressure point of the cricondentherm, cricondenbar and critical points. This then becomes the network’s output data.

In order for the network’s data to be consistent with the degree of the input data and for better understanding of the networks result, the output’s pressure and temperature were normalized. The critical condition of methane was the reference point for normalizing the pressure and temperature values of the cricondentherm, cricondenbar and critical point which is calculated by the equations given below

$$T_N = T / T_c \quad (4.5)$$

$$P_N = P / P_c \quad (4.6)$$

where,

$T_N$  = normalized temperature ( $T_N$ ) for the cricondenbar, cricondenthem and critical point

$P_N$  = normalized pressure for the cricondenbar, cricondenthem and critical point

$T$  = Temperature (K)

$P$  = Pressure (Psia)

$T_c$  = Critical temperature of methane (190.45K)

$P_c$  = Critical pressure of methane (667.19 psia)

#### 4.1.1 Neural Network Model

A neural network study is limited by how complex the relationship between the input and the output are, how fast the network architects learns this relationship, the learning algorithm being specified. Four neural networks was implemented study. The critical point, the cricondenthem, the cricondenbar, and the three coordinate network was proposed. This was used to first understand the ability of the neural network to understand the non linear relationship which exists between the natural gas compositions, specific gravity of the  $C_{7+}$  and its molecular weight with the output variable being each individual point's reduced temperature and reduced pressure of the cricondenbar, cricondenthem and the critical. The three coordinate network was then proposed for the phase envelope construction. The phase envelope points (critical point, cricondenthem and cricondenbar) neural networks were also used to predict which of these points is closely related to the phase envelope network architects in terms of complexity of

neurons. Pressure and temperature value of the cricondenbar, cricondenthem and critical of a natural gas phase envelope is more in a scattered pattern within the ranges provided for each points as shown in Table 4-3, 4-4, 4-5,. This range is further elaborated on in Fig's 4-3, 4-4, 4-5, which shows the testing and training data set for the cricondenbar, cricondenthem and critical normalized pressure and temperature values respectively. These plots were used to clarify that the networks proposed was being trained and giving results based on the network simulation rather than solving for the same points which is used for its training ( i.e. solving for the same points in both training and testing of the neural network). Showing this diversity a plot of various natural gas phase envelope's cricondenthem, critical point and cricondenbar is given in the figure below,

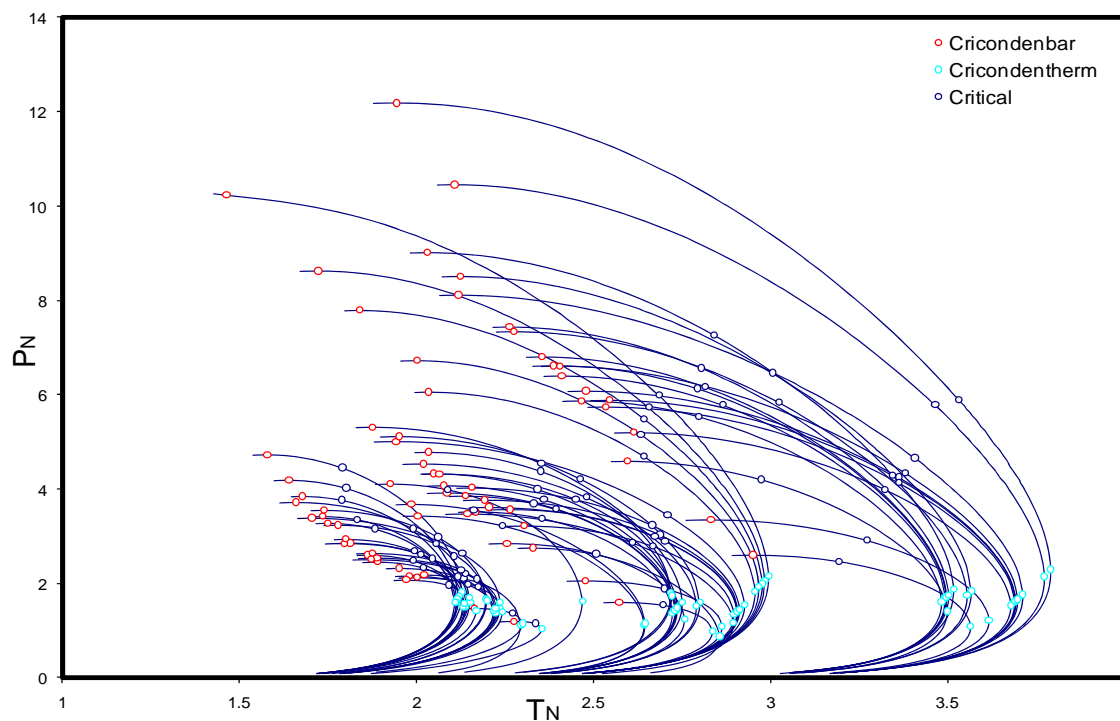


Figure 4-2: Sample of various envelopes showing distribution of pressure and temperature values

The minimum and maximum value for the normalized temperature and pressure created for the phase envelope points is shown Table 4-3, 4-4, 4-5 for the critical points, cricondenthem and cricondenbar respectively,

Table 4-3:  $P_N$  and  $T_N$  Range for Cricondenbar Neural Network

Cricondenbar	Minimum	Maximum
Normalized Pressure ( $P_N$ )	1.988	14.15
Normalized Temperature ( $T_N$ )	1.389	2.529

Table 4-4:  $P_N$  and  $T_N$  Range for Cricondenthem Neural Network

Cricondenthem	Minimum	Maximum
Normalized Pressure ( $P_N$ )	0.5775	2.595
Normalized Temperature ( $T_N$ )	1.679	3.783

Table 4-5:  $P_N$  and  $T_N$  Range for Critical Neural Network

Critical Points	Minimum	Maximum
Normalized Pressure ( $P_N$ )	0.898	11.32
Normalized Temperature ( $T_N$ )	0.82	3.518

The total 1840 data that was used for this study was divided to 1440 was used for each proposed networks training, while 400 was used for testing the networks simulation. So for each individual point of interest on the phase envelope the output points were also plotted so as to show the point distribution of the output values as shown in i.e. corresponding values of the temperature and pressure of the cricondenbar,

cricondentherm and the critical point as shown in Fig's **4-3**, **4-4**, **4-5**. This was done in order to validate the output (targets) of the network was actually learning the relationship as opposed to memorizing. And also to show that there was a distinct difference between the data that was used for training and testing of the network.

Finally comparing the all three points and the areas in which the network proposed was applicable a plot showing this was used. This plots shows that the largest area was the critical points data which is also an indication of the disparity in the values for the network which closes relates to the complexity of the network which is being proposed as shown in Fig **4-6**.

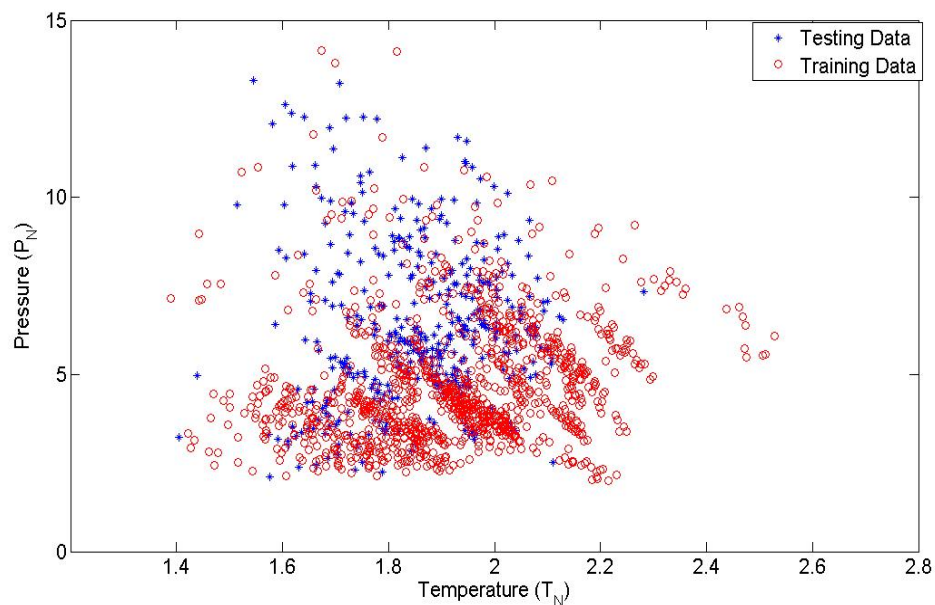


Figure **4-3**: Testing and Training Data for Cricondenbar Network Model

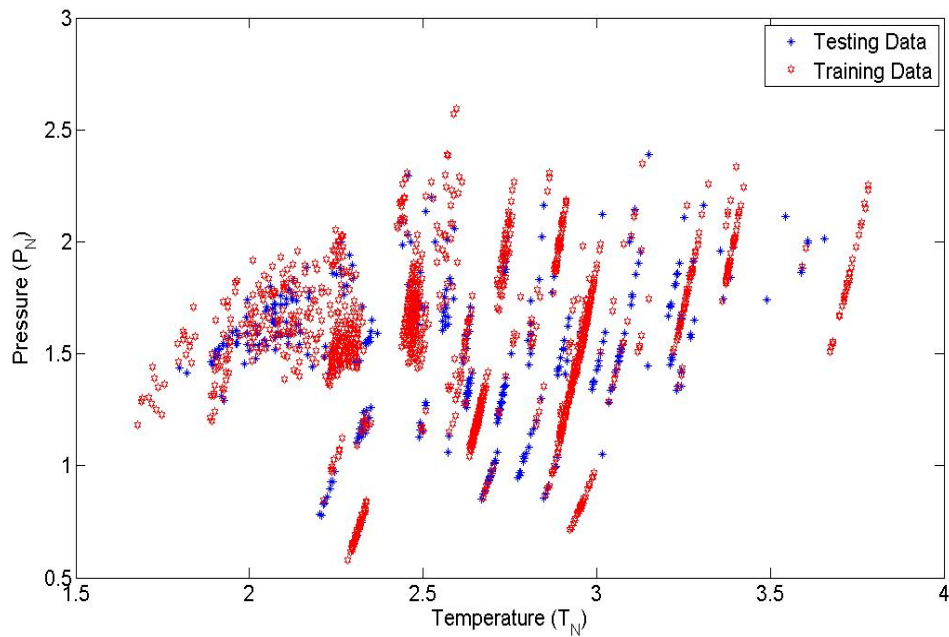


Figure 4-4: Testing and Training Targets Data for Cricondentherm Network Model

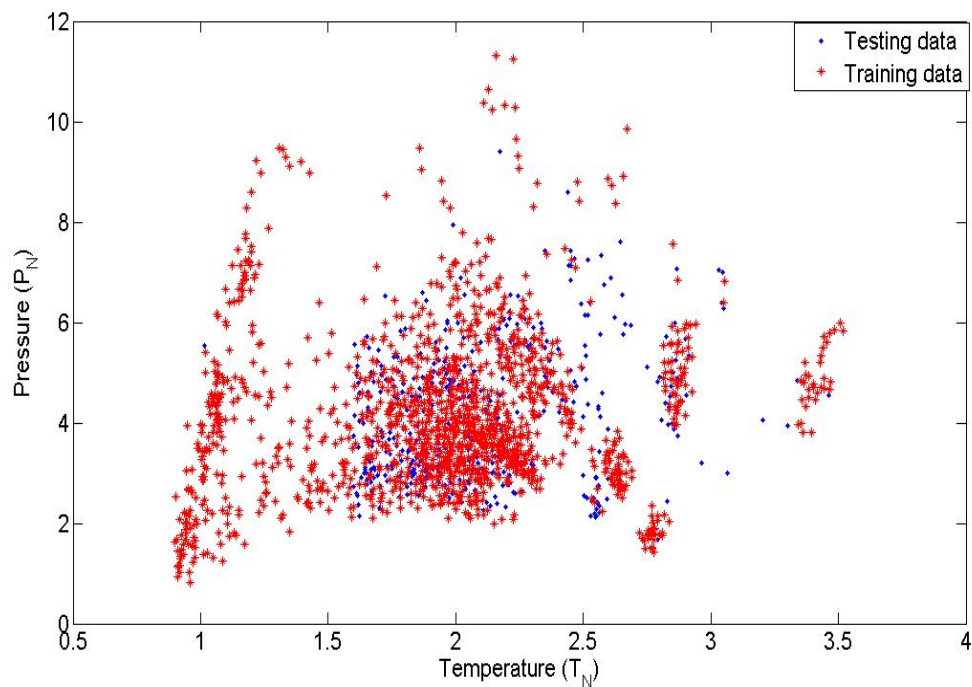


Figure 4-5: Testing and Training Targets Data for Critical Network Model

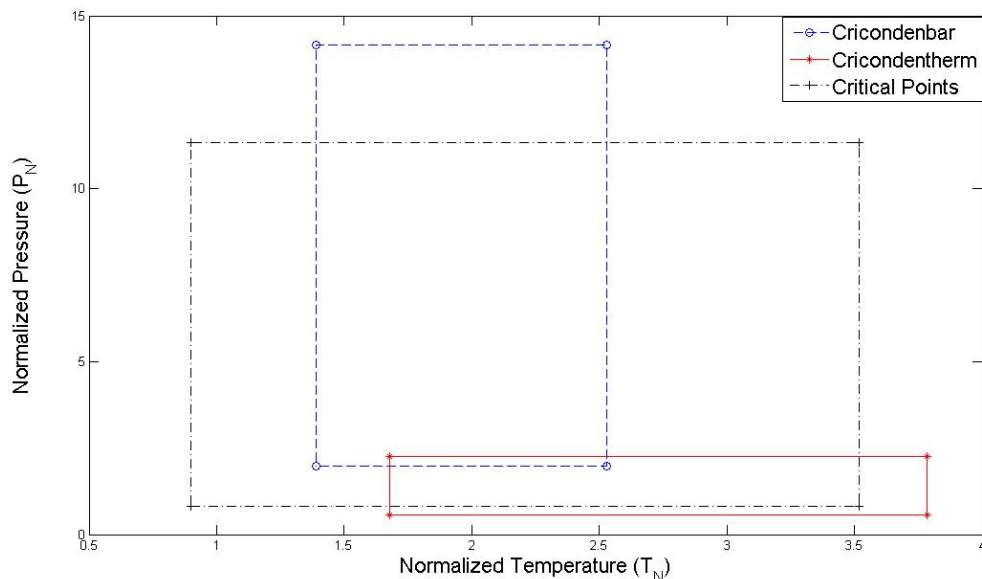


Figure 4-6: Ranges for the Temperature-Pressure 3-Coordinate Network Model

Thus the networks training and testing data set was created for inputs and output ranges. The four neural networks used the same ranges of the phase envelope characteristics for testing and training the respective neural networks. The networks proposed used the backpropagation with the newcf command. This was found to give the best result in building the network models. This created a cascade-forward network which consists of the input layer, hidden layer and the output layer. This cascade-forward network uses the weight function, input function, and the specified transfer function. The first hidden layer has weights coming from the input. Following each subsequent layer has weights coming from the input and all previous layers. All layers have biases. The last layer is which the output layer is corresponding to the targets. Also the sigmoid transfer functions were used in the training of the neural network. The two sigmoid functions used are tansig and logsig which were used in the hidden layers. While the linear transfer function (purelin transfer function) was used for the output layer.

With the data created, interchanging one of the following parameters,

- The amount of neurons used
- The number of hidden layers used
- Transfer functions specific to each layer
- Training algorithm used
- The parameters set for training to be achieved (goals, time and maximum number of epoch).

the most efficient neural network is proposed.

## Chapter 5

### Results

A neural network was trained to understand the non linear relationship between the input parameters and output parameters of an expert system whose goal was to be able to predict the pressure and temperature points of a phase envelope diagram. Composition of H<sub>2</sub>S, N<sub>2</sub>, CO<sub>2</sub>, C<sub>1</sub>, C<sub>2</sub>, C<sub>3</sub>, C<sub>4</sub>, C<sub>5</sub>, C<sub>6</sub> and C<sub>7+</sub>, with the molecular weight of the C<sub>7+</sub> (MW C<sub>7+</sub>) and specific gravity of C<sub>7+</sub> (SG C<sub>7+</sub>) were the networks input parameters. The outputs were the normalized pressure and normalized temperature of the cricondenbar, cricondentherm and the critical point. The neural network architects were used in the development of the phase envelope ANN Model for this study. Four different neural networks were proposed in this work. This work was divided into two stages. In the first stage, three different networks were modeled to predict the pressure and temperature points corresponding to the cricondenbar, cricondentherm and the critical points. The second stage was the three point's neural network in which all points corresponding to the phase envelope was utilized to be able to predict the corresponding envelope.

To evaluate the performance of each of the network the percentage of errors were compared. This error was calculated by the comparing the predicted values of the ANN Model to the actual values generated through simulation. The percentage error is calculated as

$$error\% = \frac{AA - t}{t} * 100 \quad (5.1)$$

where AA is the value predicted by the network and t in the actual input value generated by the simulation.

### **5.1 Stage One –Cricondenbar, Cricodentherm and Critical Points Network Models**

The first stage of the phase envelope neural network model study comprised of using artificial neural network to predict the pressure and temperature points corresponding of each of the points on the phase envelope which are the cricondenbar, cricodentherm and the critical points.

Stage one was developed to account for the individual points that characterizes the phase envelope which are the cricondenbar, cricodentherm and the critical point's pressure and temperature value's. This stage compares the network proposed for the cricondenbar, the cricodentherm and the critical points to each other in terms of complexity and which is most related to the 3-coordinate network for the phase envelope. This stage is sub-divided into three sections for each of the phase envelope point's neural network models. Using the composition of  $H_2S$ ,  $N_2$ ,  $CO_2$ ,  $C_1$ ,  $C_2$ ,  $C_3$ ,  $C_4$ ,  $C_5$ ,  $C_6$  and  $C_{7+}$ , with the molecular weight of the  $C_{7+}$  ( $MW_{C_{7+}}$ ) and specific gravity of  $C_{7+}$  ( $SG_{C_{7+}}$ ) as the networks input parameters. This was trained to understand each individual point's normalized pressure and temperature outputs for each respective phase envelope point. The same set of data was used for both stage studies.

The analysis and results of the respective neural networks in this stage are given in sections **5.1.1**, **5.1.2** and **5.1.3** for the cricondenbar, cricodentherm and critical point neural network respectively.

### 5.1.1 Cricondenbar Neural Network

In training neural network for the cricondenbar's pressure and temperature points, network of four layers was created. The MATLAB code created is given in Appendix A. The architect implemented 12 input neurons, and had two hidden layer with 15 neurons in each layer as shown in neural network architect in Fig 5-1.

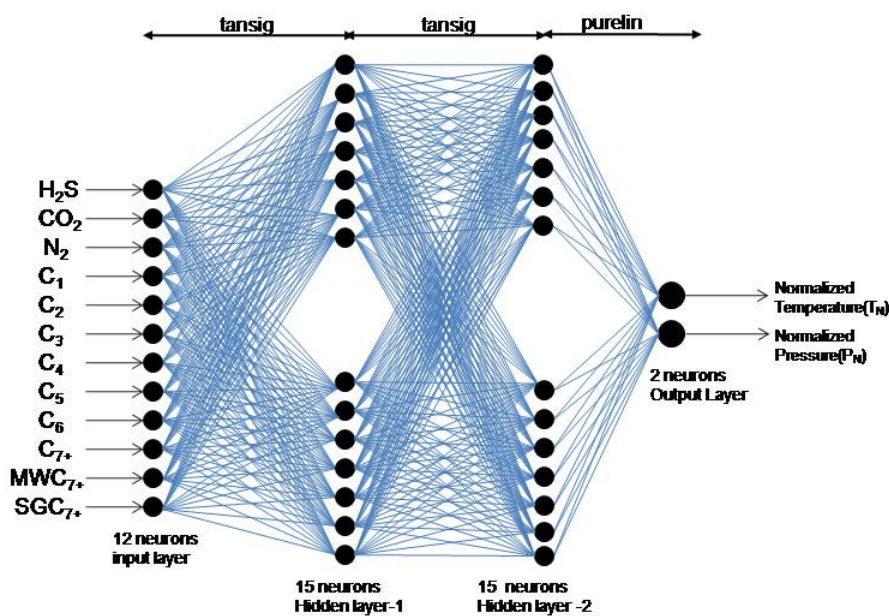


Figure 5-1: Neural Network Architect for Cricondenbar's Training and Testing

Fig 5-1 shows the input parameter were the composition of  $H_2S$ ,  $N_2$ ,  $CO_2$ ,  $C_1$ ,  $C_2$ ,  $C_3$ ,  $C_4$ ,  $C_5$ ,  $C_6$  and  $C_{7+}$ , with the Molecular weight of the  $C_{7+}$  ( $MW C_{7+}$ ) and specific gravity of  $C_{7+}$  ( $SG C_{7+}$ ). The normalized pressure and temperature of the cricondenbar was the

output layer for the network model. The total data used for this network was 1840 natural gas compositions. As earlier stated 1440 was used to train the network and 400 was used for testing the network model. The final result of the expert system is presented in Fig 5-2 and Fig 5-3,

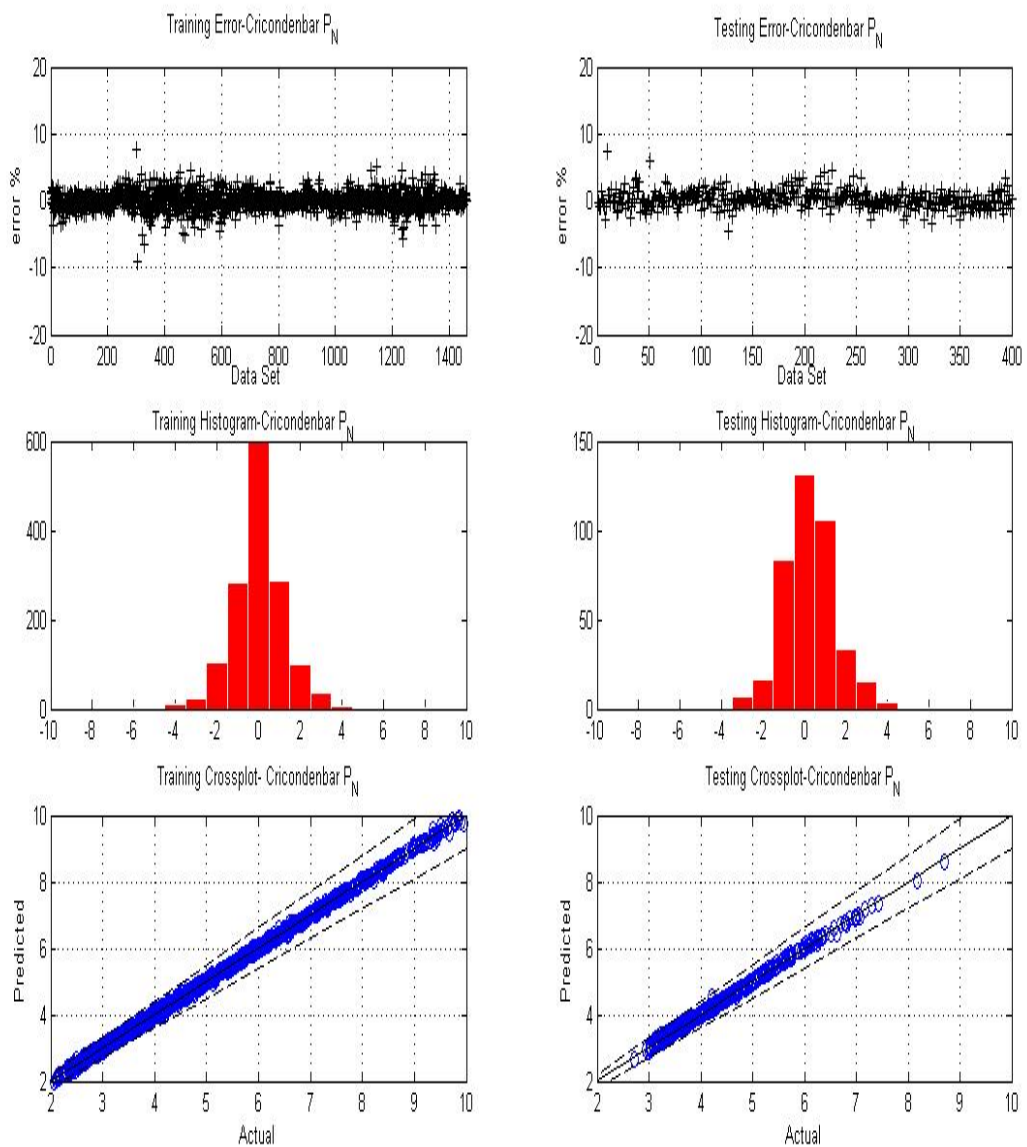


Figure 5-2: Training (left) and Testing (right) Result Plots for the Normalized Pressure of Cricondenbar Points

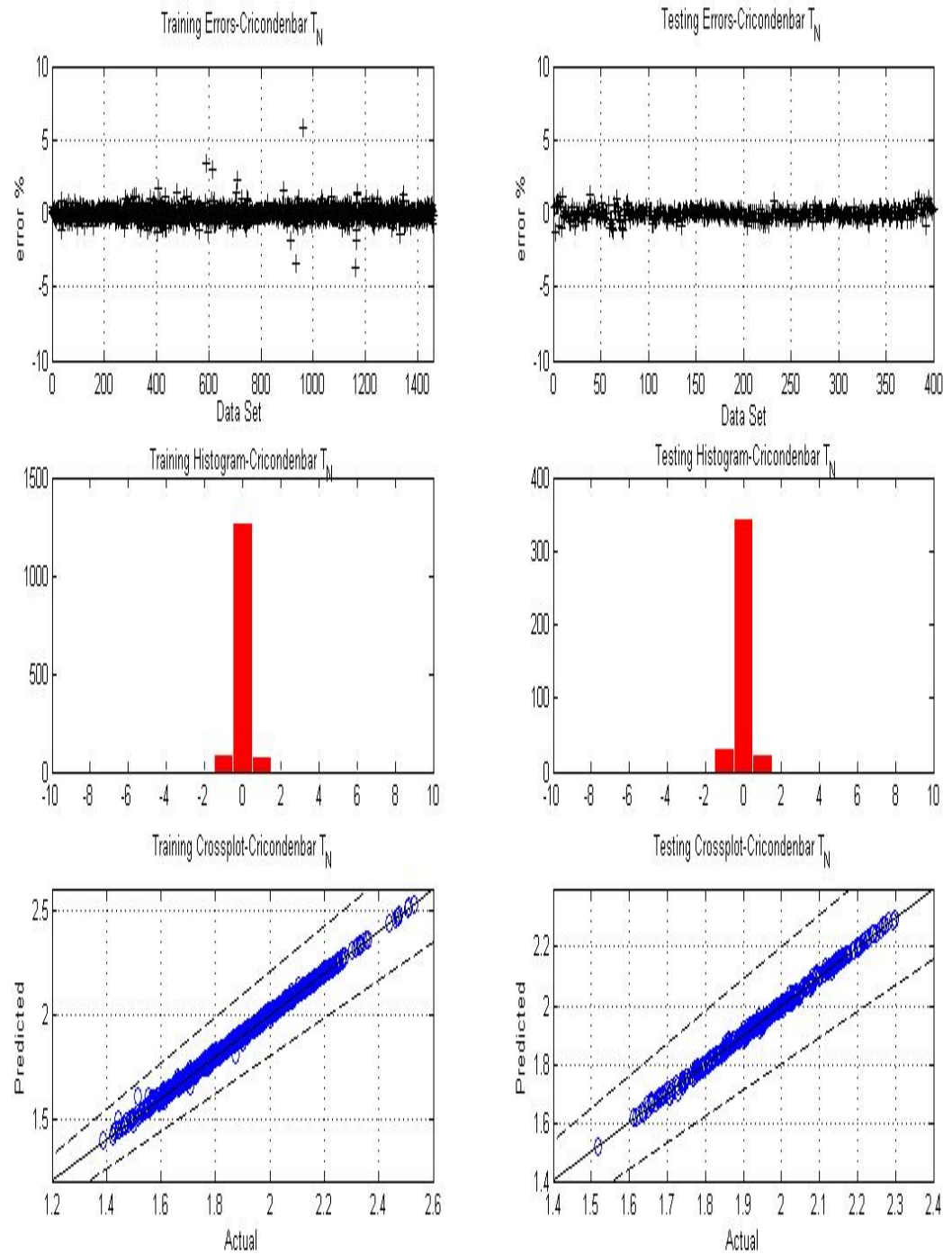


Figure 5-3: Training (left) and Testing (right) Result Plots for the Normalized Temperature of Cricondenbar Points

It could be seen from Fig 5-2 and Fig 5-3 above that this network is capable of predicting the corresponding values of pressure and temperature with the average error less than +/- 4%, which is a good indication that of the strength of this network. In analyzing this expert system three different plots were used. An error percentage, a histogram error plot and finally, a plot of the actual versus predicted whose values are supposed to be centered on the unit slope line (which is the crossplot). The percentage error plot was used in comparing the actual percentage of the error being calculated and which ranges the error being calculated were. The histogram is particularly useful in depicting what ratio the error percentage is being distributed. The histogram shows the frequency of the error being calculated. Ideally, the highest frequency should be zero for an accurate expert system. Verifying the results further a cross plot is used. This is a plot of the predicted and the actual centered on a 45° slope line. This is used as a reference of the error deviation. A +/-10 % line was introduced to the crossplot which acts as a boundary line for the 45° slope line in comparing the errors of the final result. This was done in order to get a better approximation of the error calculated for the result as it was seen to be scattering above even the 10% for the some network prediction. For a perfect trained network the points should be found on this line or as close as possible (45° slope line).

It could be seen that with this model presented that the error results were indeed moderate for the normalized temperature and pressure corresponding to the cricondenbar. This network thus is a good predictive tool for the highest point of pressure value on a phase envelope plot i.e. cricondenbar points for pressure and temperature. This model is shown

to be applicable to the composition values within the ranges provided in Table 4-3. Also the relevancy of the input which is used for the training of this network was investigated. For this analysis the relevancy proposed by Belue and Bauer (1995) is used where the relevancy input is calculated by Eq. (5.2) given below,

$$S_i = \sum_{j=1}^n |s_{ij}|, \quad (5.2)$$

where  $S_{ij}$  represents the weight of relevance of input  $I$  on neuron  $j$  of the first hidden layer and  $n$  is the number on neurons the relevancy of each input in the architect proposed for the cricondenbar is given in Fig 5-4.

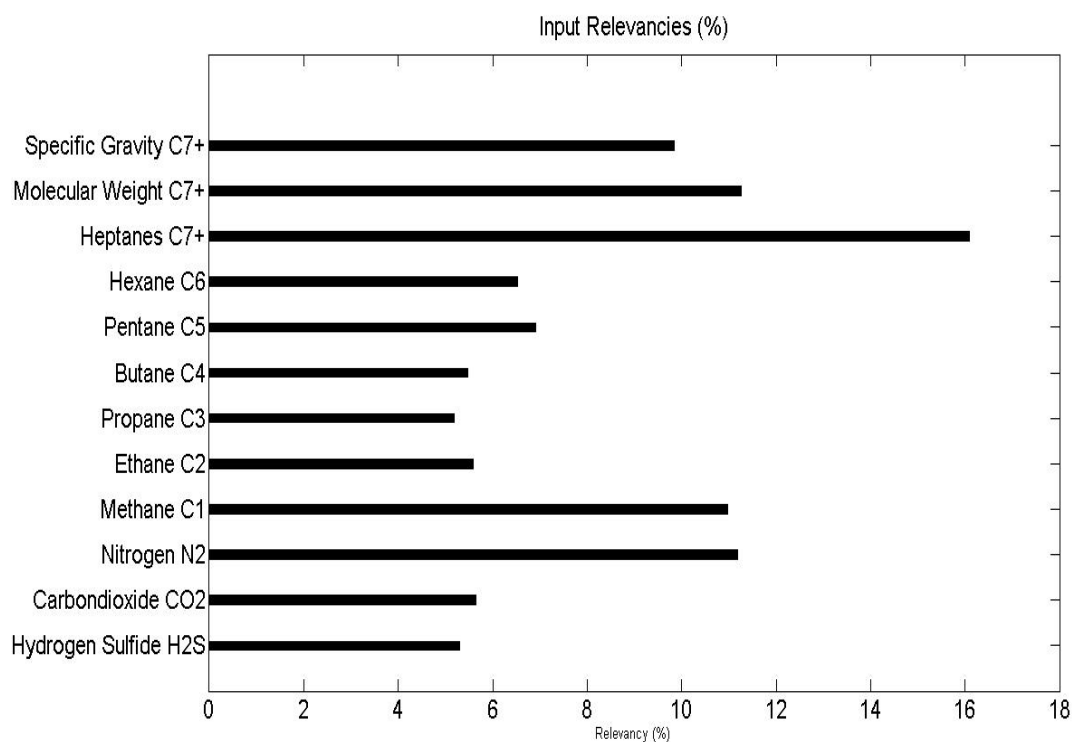


Figure 5-4: Relevancy for each input for Cricondenbar

It can be seen from the plots that the heavy fraction ( $C_{7+}$ ) composition and the properties had a large influence on the cricondenbar neural network's prediction. Also the methane ( $C_1$ ) and the nitrogen ( $N_2$ ) which is an impurity had a considerable large influence on the neural network with approximately 11.3% and 11.7% respectively. The  $CO_2$  and  $H_2S$  which are the other impurity present in this reservoir fluid had an influence which was less than 6%.

Concluding from the results of the cricondenbar expert system, it is capable of predicting the temperature and pressure of natural gas composition.

### 5.1.2 Cricondenthem Neural Network

After analyzing the neural simulation study, a neural network which utilizes two hidden layer was found to be the best for the cricondenthem expert system. This neural network model for the cricondenthem pressure and temperature the network uses four layers. The architect used 12 input neurons for the input layer, and had two hidden layer with 10 neurons in each layer followed by two output neurons. This architect used the logsig transfer function for the first two layers. The outer layer transfer function was purelin. This network's combination of neurons and the transfer's functions were found to be the best combinations for the temperature and pressure values prediction for the cricondenthem points. The proposed expert system's architect is shown in Fig 5-5.

The same set of plots that were used for the analysis of the cricondenbar neural network model was used here to analysis the proposed cricondenthem's expert systems performance. The error percentage plot, the histogram plots and the cross plot. The three

different plots showing the variation of the error being obtained by the network architect.

The results of the expert system are given in the subsequent Fig 5-6 and Fig 5-7.

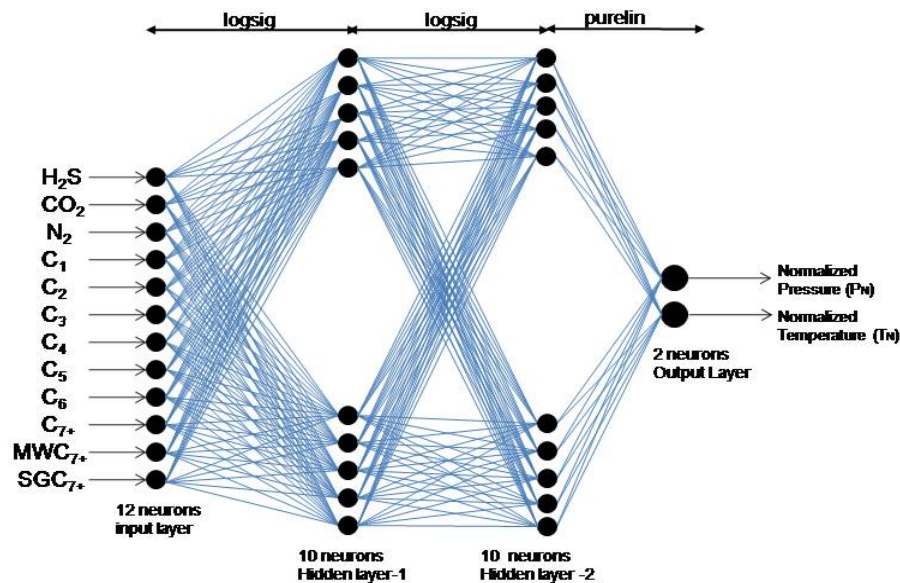


Figure 5-5: Neural Network Architect for Cricondentherm's Training and Testing

This neural network architect's plot shown above produces error within an acceptable range of less than 3% for testing and training data range which was used. It can be seen that the expert systems histogram barely had error calculated other than zero which is a good indication of the accuracy of the network model. The range of the cricondentherm pressure and temperature value which this network is applicable is shown in Table 4-4.

Also obtained was the relevancy of the input of data set on the networks model which is given in Fig 5-8.

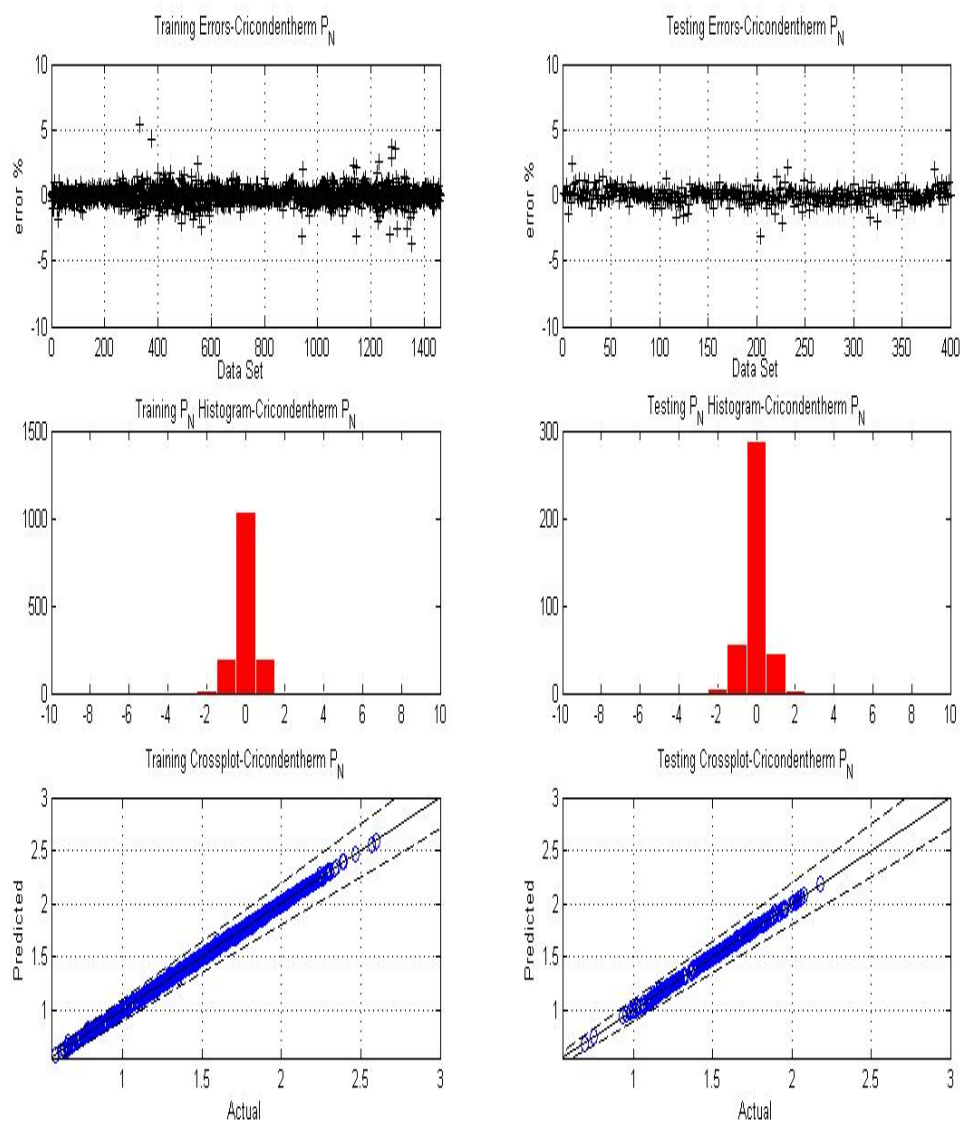


Figure 5-6: Training (left) and Testing (right) Result Plots for the Normalized Pressure of Cricondentherm Points

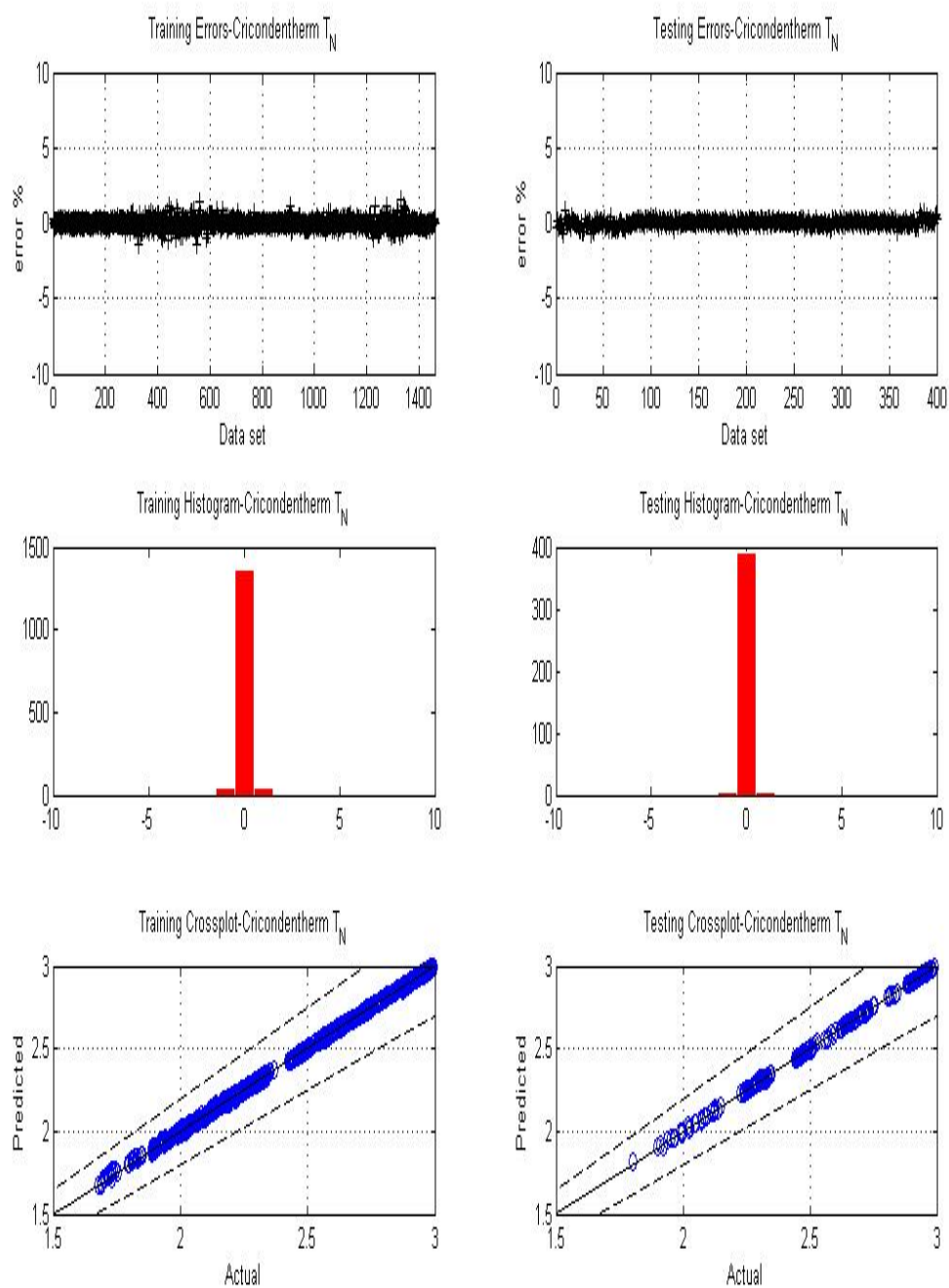


Figure 5-7: Training (left) and Testing (right) Result Plots for the Normalized Temperature of Cricondentherm Points

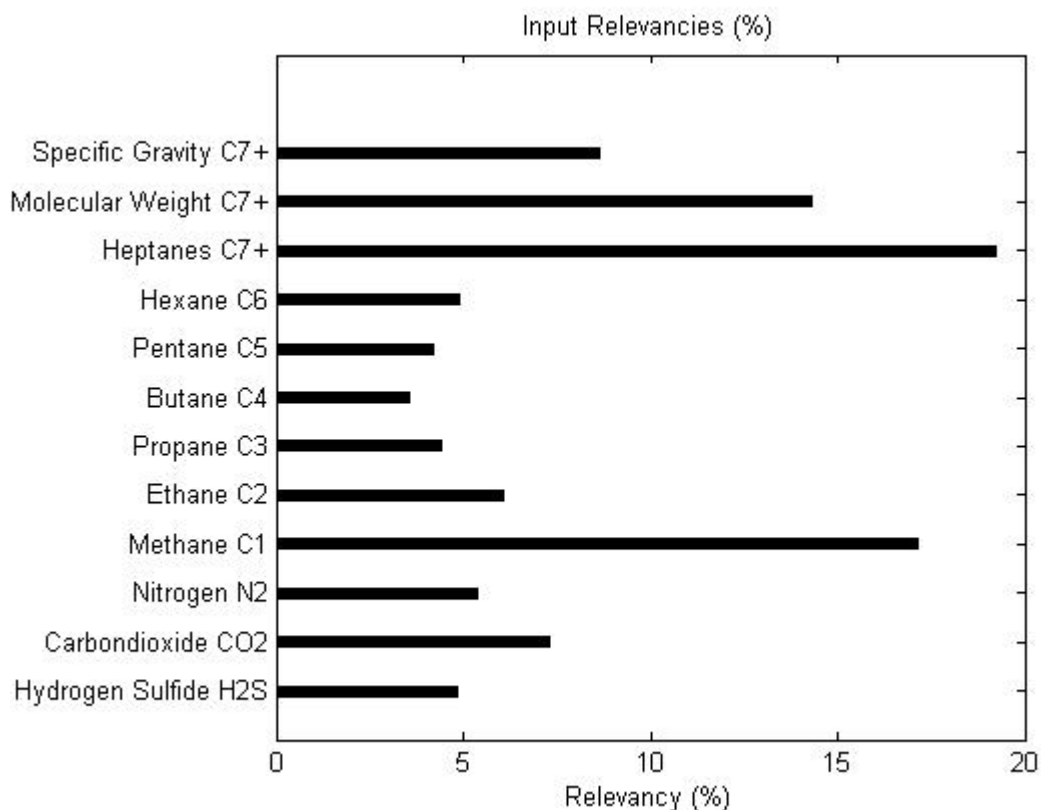


Figure 5-8: Relevancy percentage for the Cricondentherm neural network

It can be seen from the relevancy plot that the most predominant in the network model prediction was the composition ( $C_{7+}$ ). The methane  $C_1$  composition and the molecular weight of the ( $C_{7+}$ ) had a great influence on the models compared to other input parameter. The nitrogen did not have as much influence on the cricondentherm's model as in the case of the cricondenbar neural network model.  $H_2S$  had a similar influence which was approximately 5% but comparing the total impurities influence the cricondentherm neural network had a lesser influence on the model prediction than that of the cricondenbar neural network.

This expert system can be seen to predict the pressure and temperature within a very reasonable error percent ranges. The range for the error was well within [+2% -2%] for both the pressure and temperature value for the range of the natural gas composition used for this study.

### 5.1.3 Critical Neural Network

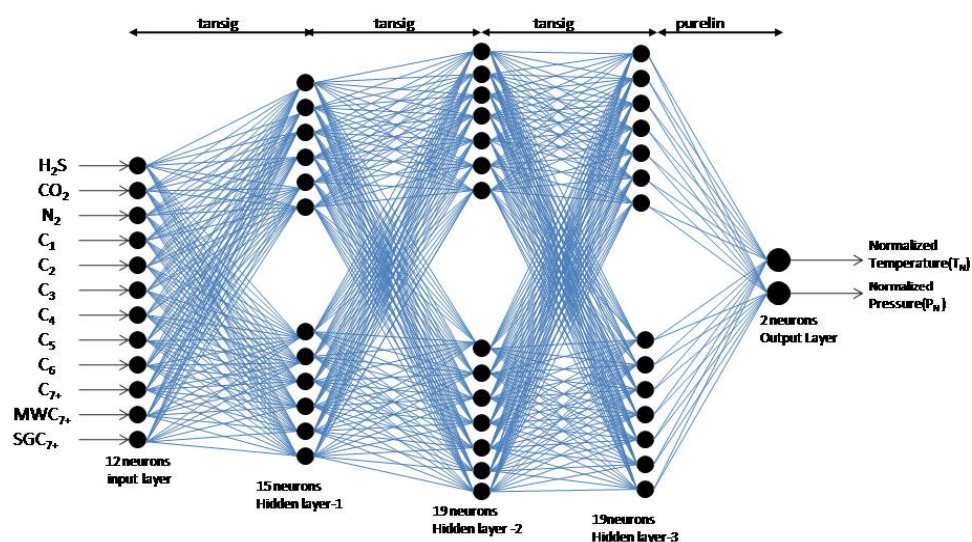


Figure 5-9: Architect for the Critical Neural Network

A three hidden layer network as shown in the network architect in Fig 5-9 was most efficient for the critical point neural network. This gives the best results with the least of the error calculation in prediction of the pressure and temperature value of the critical point's, this was achieved after a series of different types of transfer function and amount

of hidden layer to find which is most optimum combination. The network proposed utilizes 15 neurons in the first hidden layer and 19 neurons each in the second and third hidden layers. It was also found out that the tansig transfer function was best fit for the training and testing of this network of all the layers in the network. The results plots of the network model is given in Fig 5-10 and Fig 5-11,

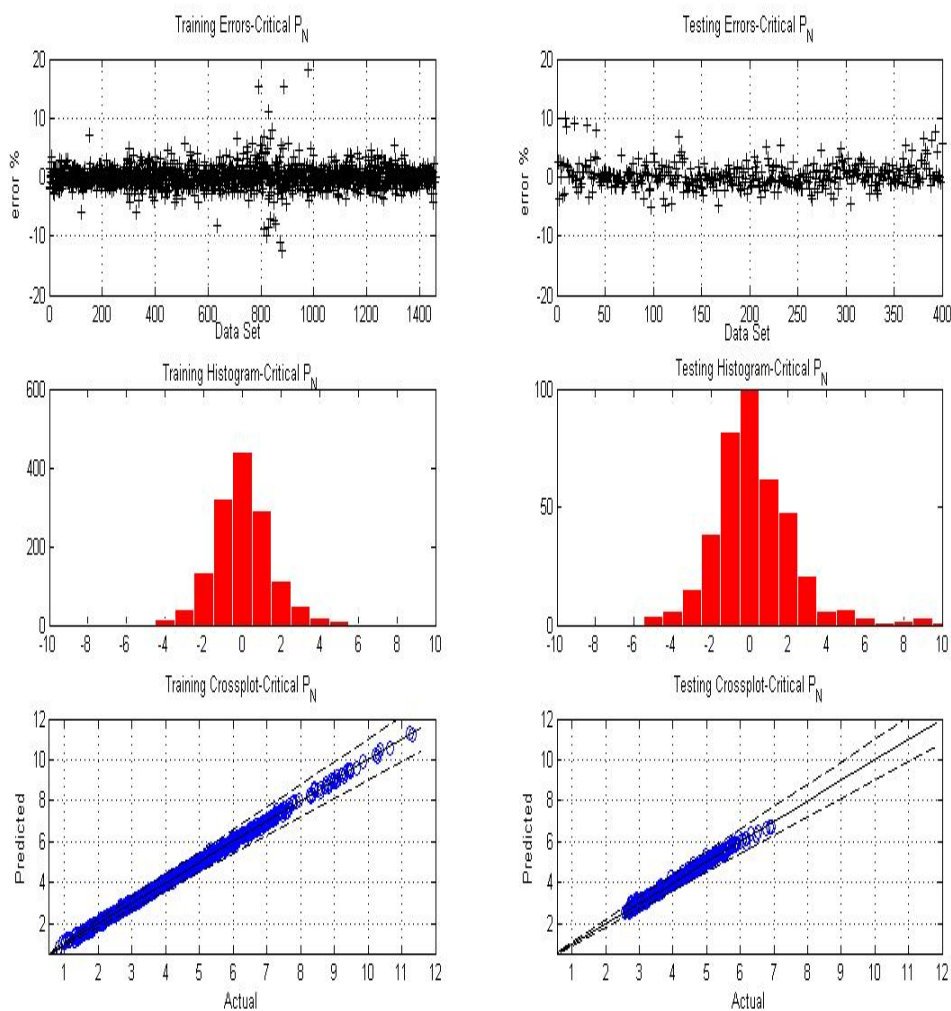
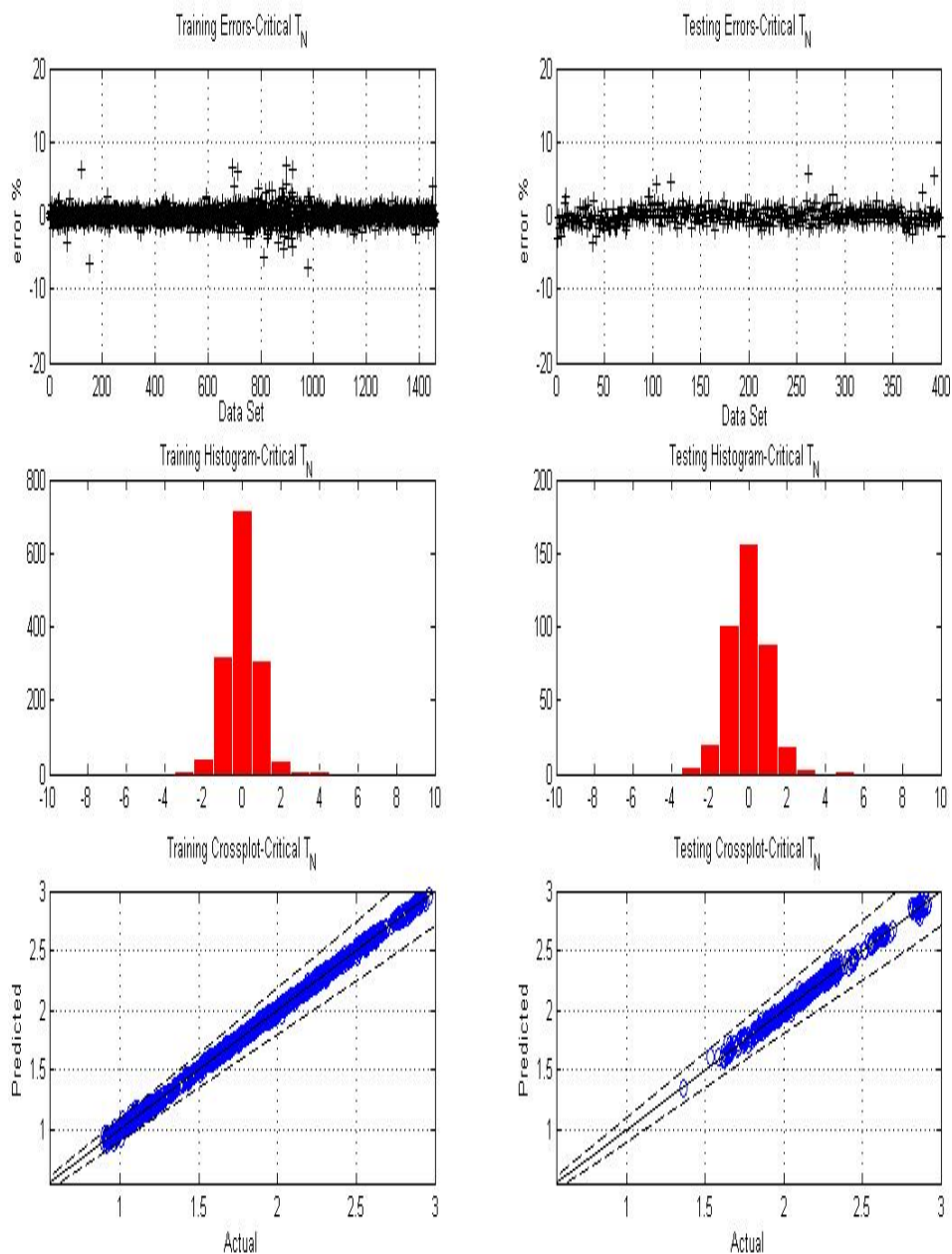


Figure 5-10: Training (left) and Testing (right) Result Plots for the Normalized Pressure Points of Critical Points



**Figure 5-11:** Training (left) and Testing (right) Result Plots for the Normalized Temperature of Critical Points

The critical point was the most complex model comparing the three points of the neural network model points developed individually. This network utilized a three hidden layer network to understand this relationship. The tansig transfer function was used in the three hidden layer with the purelin at the output layer. It could be seen from the plot that the error predicted were still moderate even thou the results were not as good as the cricondentherm or the cricondenbar's model. Also the relevancy which is given below in Fig 5-12, shows that the highest still remain the heavies  $C_{7+}$  which is in the range of 15.5% followed by the nitrogen  $N_2$  with a percentage of approximately 11%. The impurities had similar influence compared to the cricondenbar neural network.

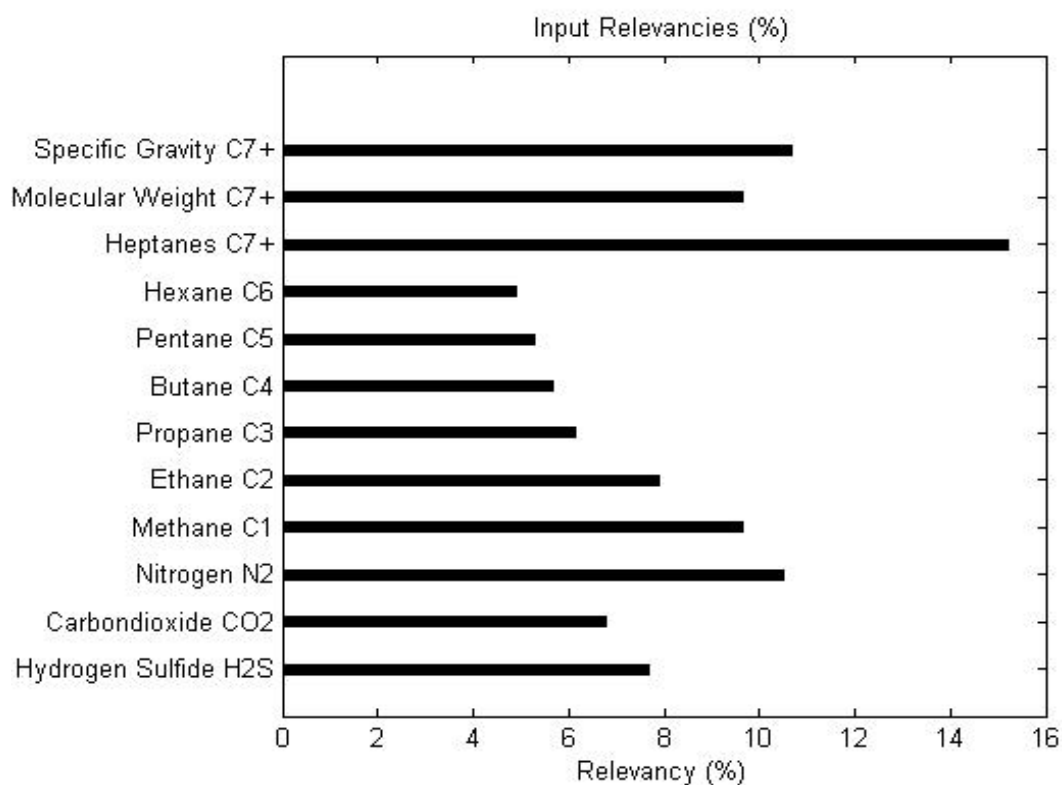


Figure 5-12: Relevancy Percentage for the Critical Neural Network

## 5.2 Stage Two- 3-Coordinate Neural Network

The 3-coordinate points which define the phase envelope neural network model is presented in the stage two of this ANN model study. Stage two consisted of finding a neural network which integrates all the three main points of the diagram in one model. This neural network should be able to predict the corresponding temperature and pressure value of the cricondenbar, cricondenthem and the critical point. The proposed network for this which gives the best results for the phase envelope points is given in Fig 5-13,

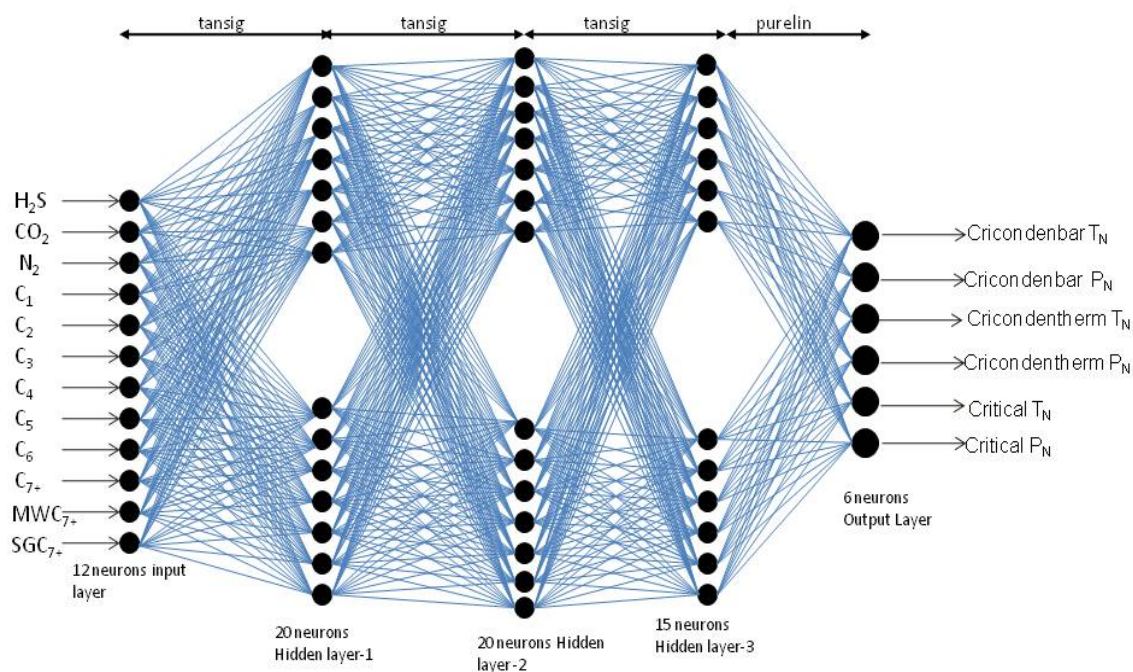


Figure 5-13: Phase Envelope Neural Network Architect

As shown in Fig **5-13** the input parameter were the composition of  $H_2S$ ,  $N_2$ ,  $CO_2$ ,  $C_1$ ,  $C_2$ ,  $C_3$ ,  $C_4$ ,  $C_5$ ,  $C_6$  and  $C_{7+}$ , with the Molecular weight of the  $C_{7+}$  (MW  $C_{7+}$ ) and specific gravity of  $C_{7+}$  (SG  $C_{7+}$ ). And the output parameters being the normalized pressure and temperature of the cricondenbar, cricondenthem and critical point values were the networks output layer for the 3-coordinate neural network model.

The phase envelope neural network utilizes a three hidden layer network. This network uses 20 neurons in the first and second hidden layer. The final hidden layer has 15 neurons. This network used the tansig transfer function in the three hidden layer and a purelin transfer function in the output layer. This was achieved using the ANN toolbox developed by MATLAB. Details about the MATLAB code can be found in Appendix B. The result analysis was similar to the set utilized in the stage one of this study. This uses the error percentage plot, histogram plot and the crossplot of the actual versus the predicted. The results analyzed each of the pressure and temperature points of the cricondenbar, cricondenthem and the critical point individually. These results are presented in Fig's **5-14** to **5-19** below for each respective points of the three coordinate neural network proposed.

A relevancy study was also used to determine the ratio of each of the input parameter to the 3-coordinate network model (phase envelope ANN) which is presented in Fig **5-20**.

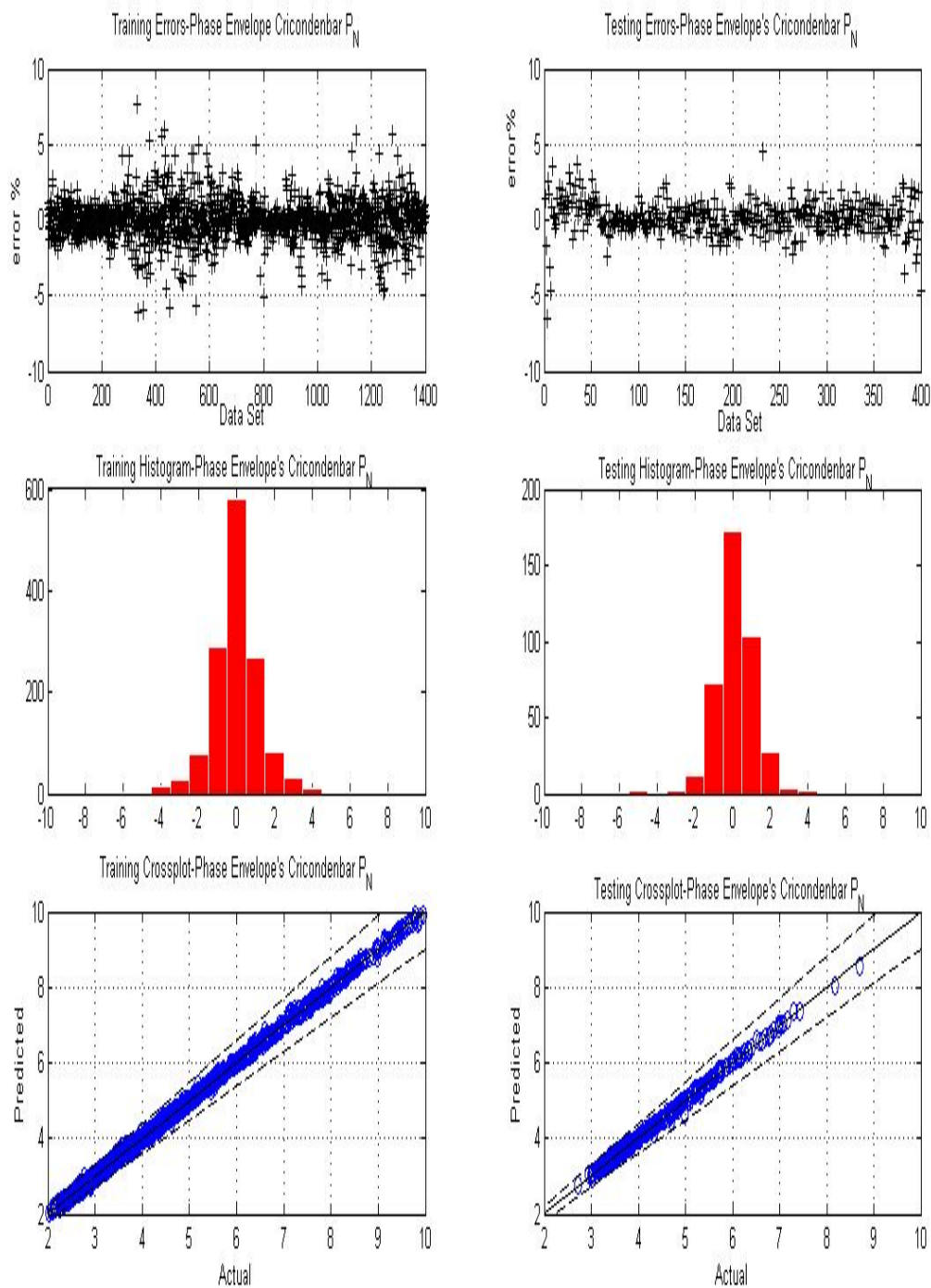


Figure 5-14: 3-Coordinate Cricondenbar Training (left) and Testing (right) Pressure Results Plots

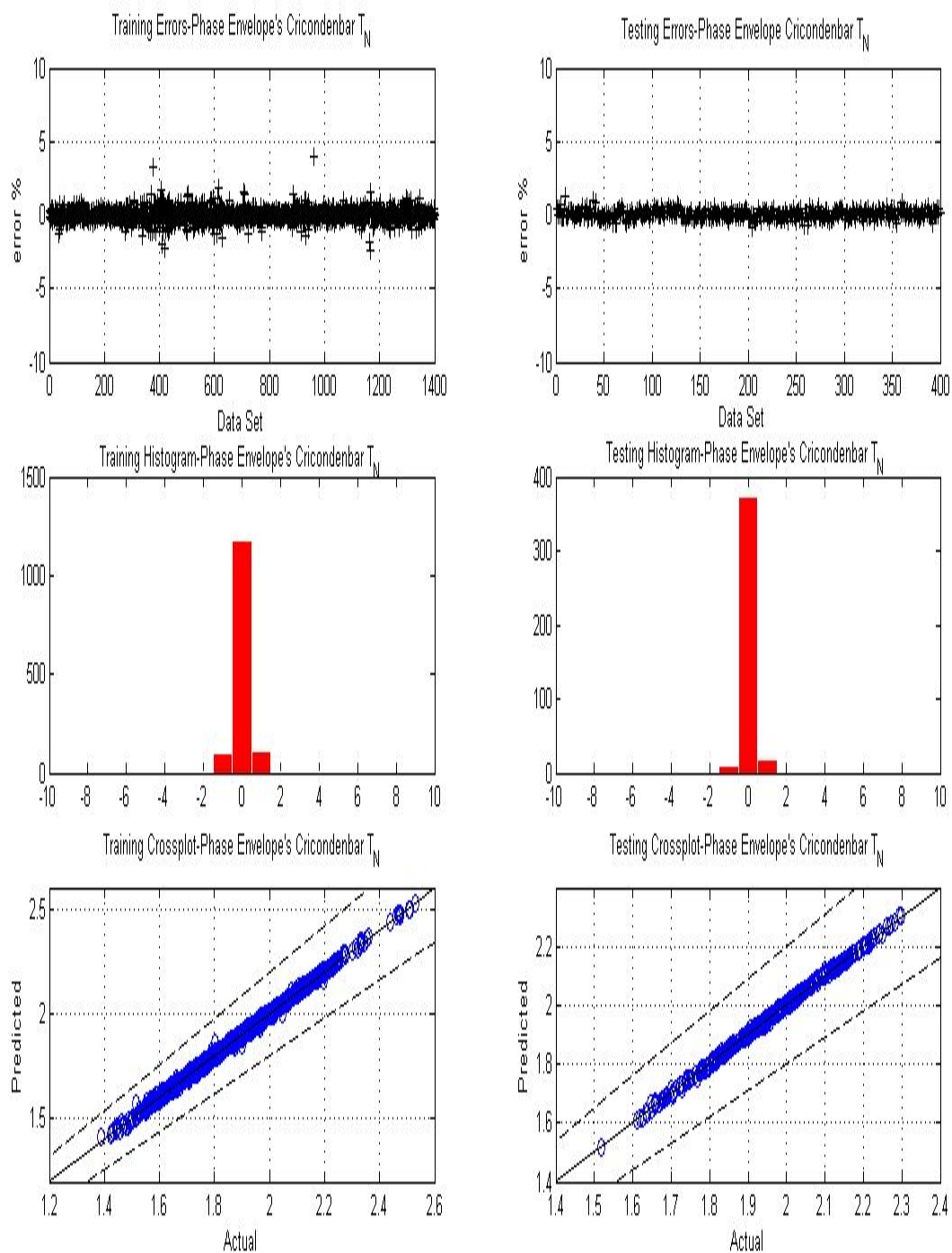


Figure 5-15: 3-Coordinate Cricondenbar Training (left) and Testing (right) Temperature Results Plots

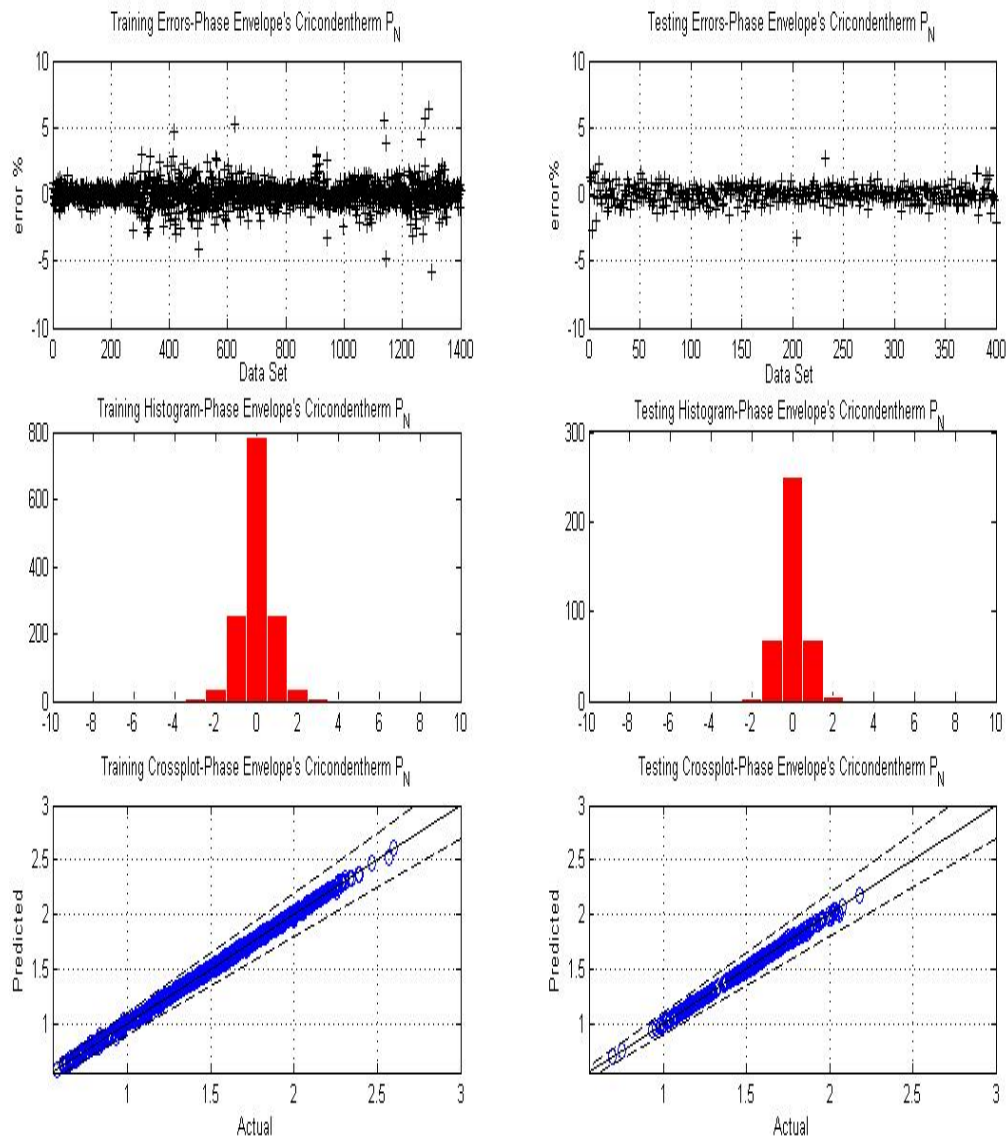


Figure 5-16: 3-Coordinate Cricondentherm Training (left) and Testing (right) Pressure Results Plots

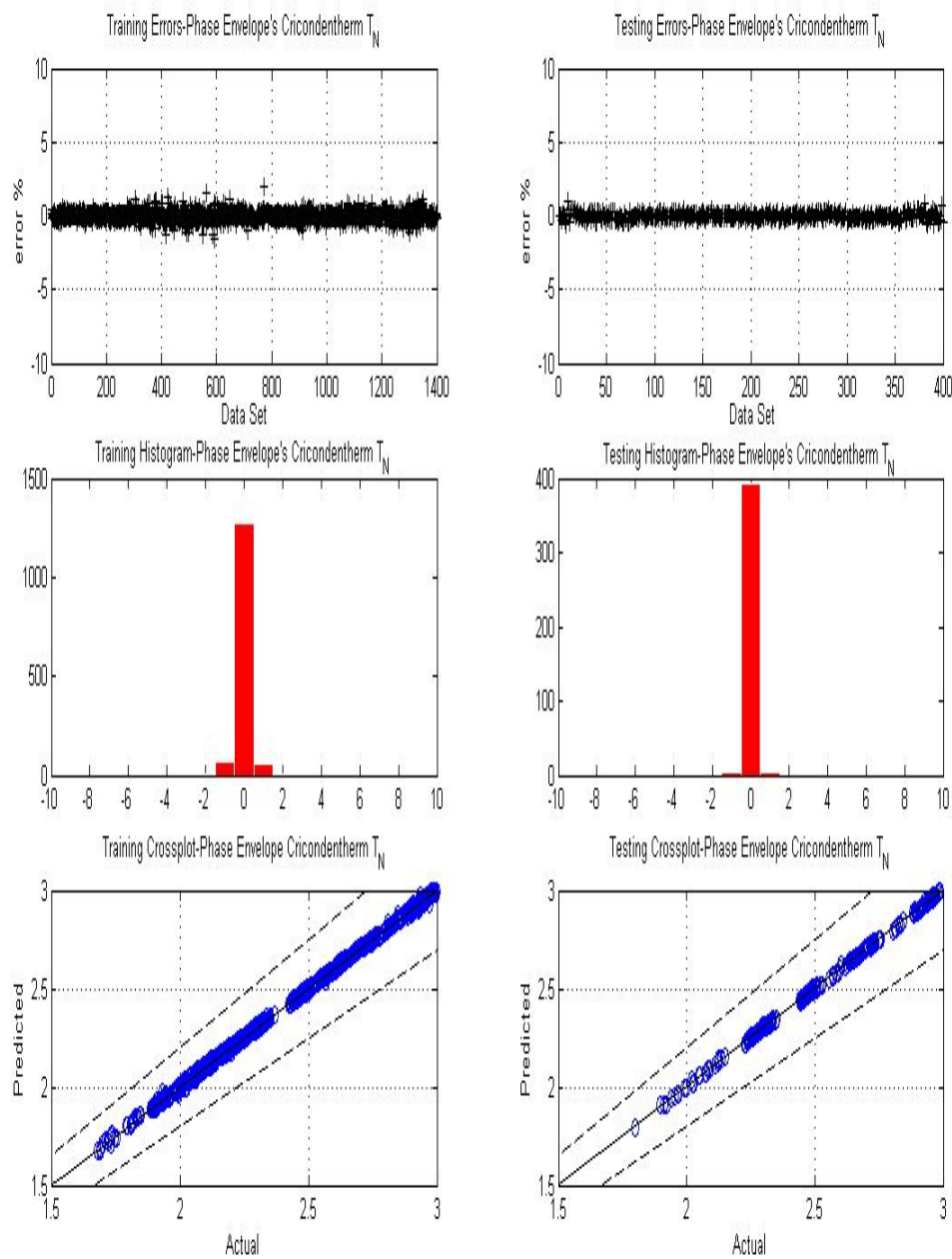


Figure 5-17: 3-Coordinate Cricondentherm Training (left) and Testing (right) Temperature Result Plots

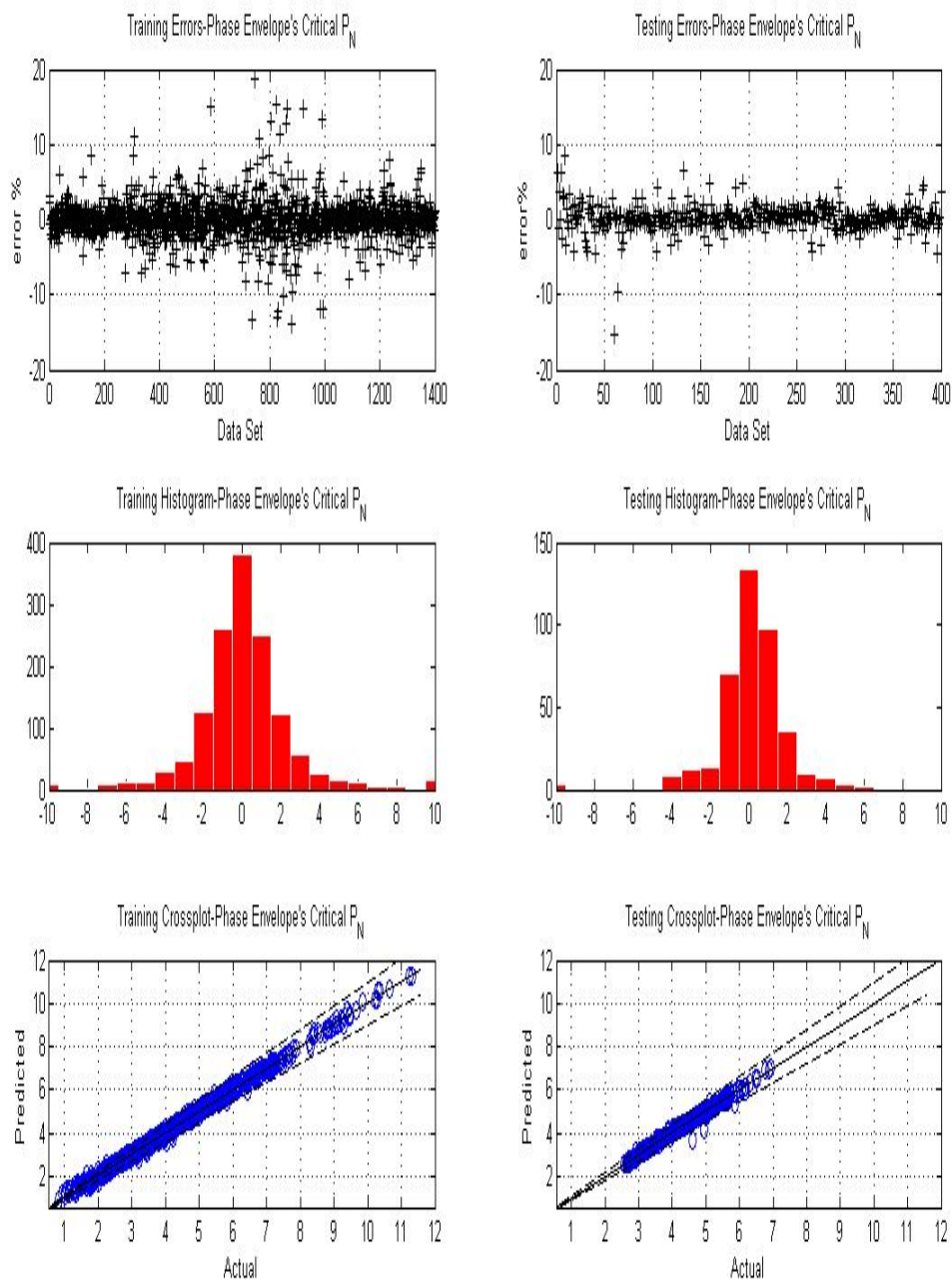


Figure 5-18: 3-Coordinate Critical Training (left) and Testing (right) Pressure Result Plots

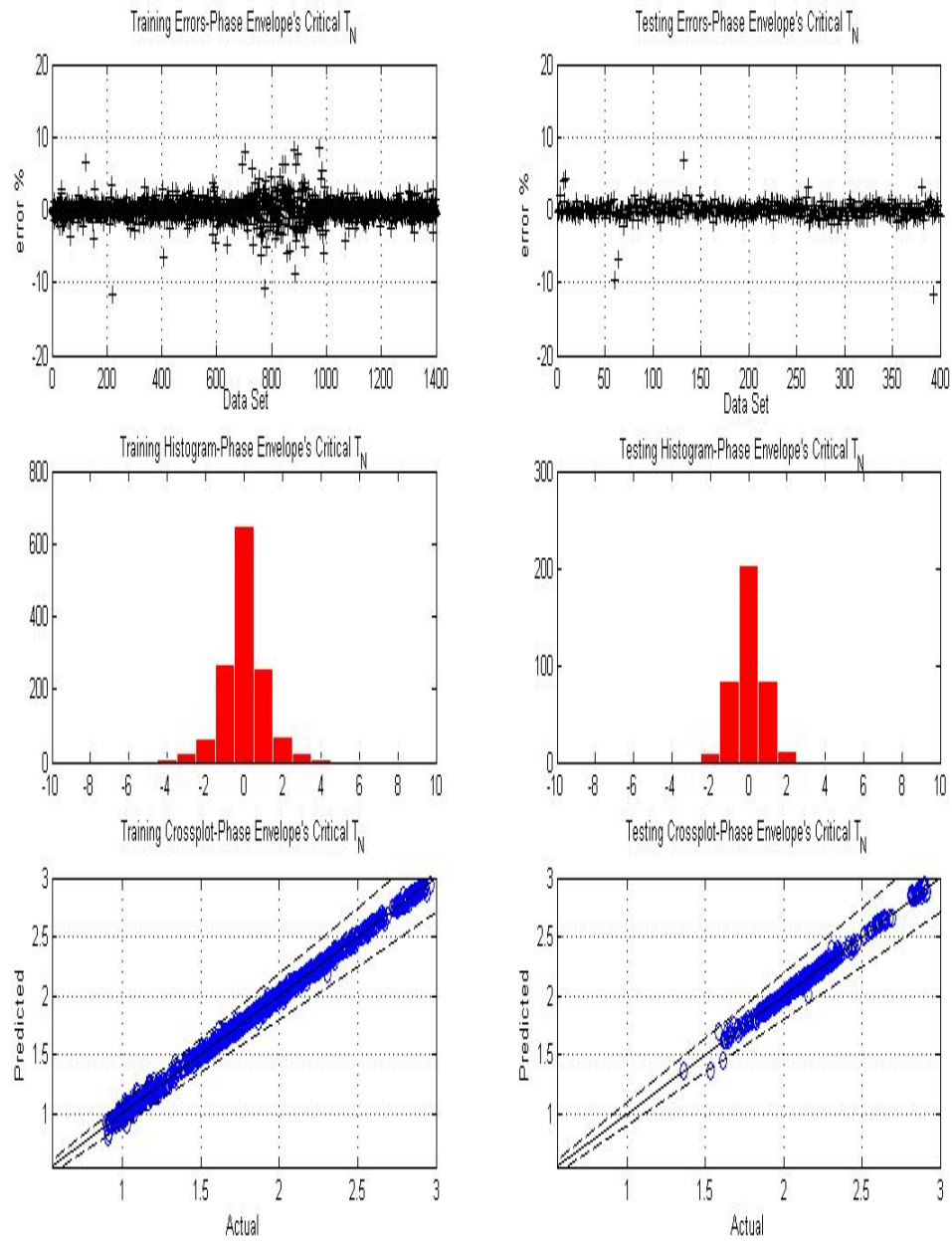


Figure 5-19: 3-Coordinate Critical Training (left) and Testing (right) Temperature Result Plots

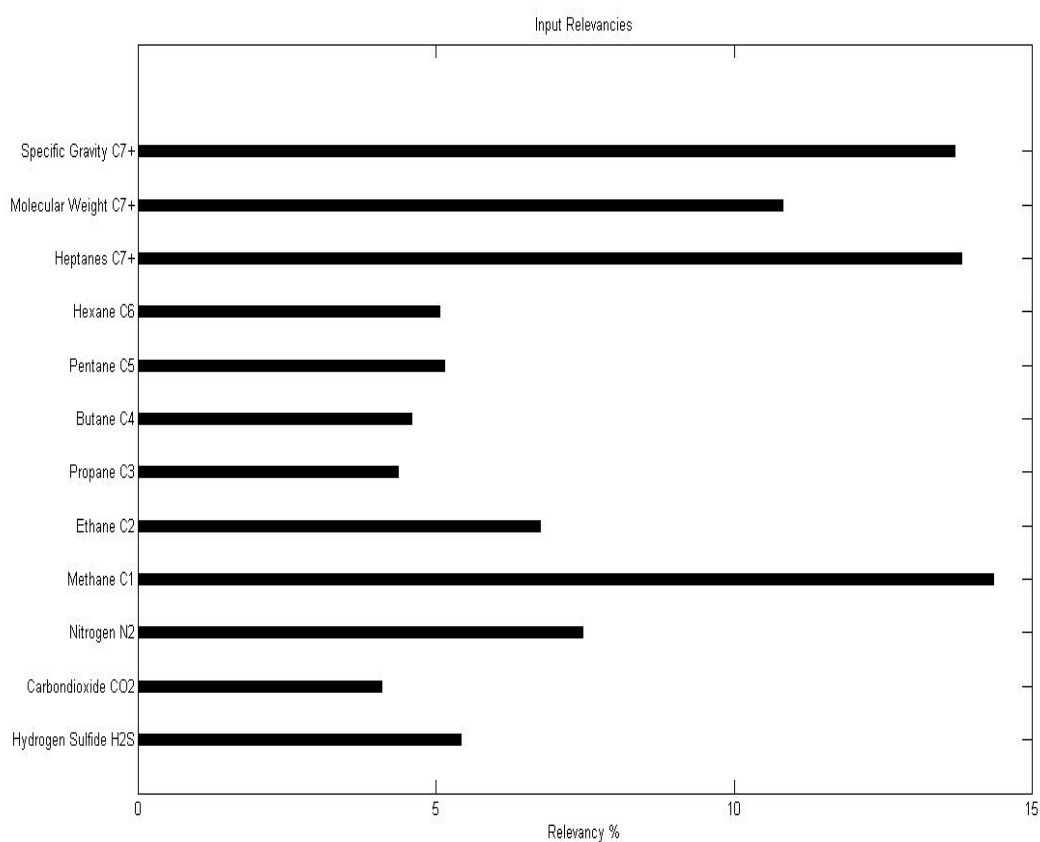


Figure 5-20: Relevancy Plot for the Phase Envelope Input

It can be seen from the results in this stage that the 3-coordinate neural network produced similar results to the ones in stage one. This network is able to predict the corresponding temperature and pressure of the cricondenbar and the cricondentherm and the critical point for the ranges of natural gas mixture which were used for this study. Also, all inputs parameter had a relevancy in the phase envelope prediction. The highest relevancy was the compositions of methane  $C_1$  and  $C_{7+}$  with 14%, while the specific gravity of the  $C_{7+}$  was approximately 13.7%. The impurities had a total of 17% on the network prediction.

## Chapter 6

### Summary and Conclusion

A powerful tool has been developed using artificial neural network which is capable of predicting key phase envelope points which are the cricondenbar, cricondenthem and critical point pressure and temperature of natural gas composition provided that the composition analysis data is available. Also developed is a tool which estimates the pressure and temperature value of the points which defines the phase envelope individually. The study examined in two stages. The first three neural networks were developed to investigate the ability of artificial neural network in prediction of these individual points on the phase envelope. A total of 1840 different mixture composition was used in training and testing each of the neural networks proposed. It can be seen from the plots that the best results was the cricondenthem pressure and temperature points and also the easiest which requires the least complex network architect. The histogram plot shows error calculate was between the range of [-2% +2%] for the cricondenthem pressure while cricondenthem temperature was between [-1% +1%] for both the testing and training results. The cricondenbar pressure on the other hand although needing a more complex network which utilized an extra layer of neuron more than the cricondenthem network model to achieve the desired results had similar network performance. The error range for the cricondenbar pressure training error was within [-4% +4%] and testing was [-3% +4%]. Cricondenbar temperature also had the same error range as the cricondenthem which was [-1% +1%] for both the testing and

training the network model. This shows that the neural network models for the natural gas mixtures can effectively predict the cricondenthem and cricondenbar point.

For the critical point error results were slightly higher for both the temperature and pressure values. The temperature point were predicted with errors within +/- 5% for both testing and training, while the critical pressure prediction was in [-5% +10%] error margin.

The second stage was developing a 3-coordinate neural network which represents the three points defining the shape of the phase envelope. Using the histogram plot for result analysis, the error calculated for the cricondenbar pressure training was in the range of [-4% +4%] while the testing data was predicted with error calculated in the range of [-5% +4%]. The cricondenbar temperature error for testing and training were calculated within [-1% +1%]. The cricondenthem point had error less than the cricondenbar points predicted for the neural network proposed. The cricondenthem pressure training was calculated error was in the range of [-3 +3%] while the cricondenthem temperature testing and training error was [-1% +1%]. The critical point value was predicted with a higher percentage error when compared to the other two points of the 3-coordinates network model. The critical points pressure training was in the range of [-10% +10%] and the testing was calculated in the range of [-10% +10%]. The critical point temperature values training was in the range [-4% +4] and testing error was [-2% +4%].

The 3-coordinate network model was able to match the training and testing error percentage for the three points which defines the phase envelope when compared to the individual neural network model developed in the first stage.

It was also noticed that the temperature values for each of these points were predicted with lesser error than the pressure values of all points. The  $C_{7+}$  composition was consistent in the relevancy of both stages model proposed.

The neural network proposed gives a fast and reliable way in which phase envelope could be estimated with minimum error for the points defining the shape. These model proposed network shows very promising result for further related work. The model could be improved by introducing additional data in which the model is trained with (i.e. experimental data). An infusion with experimental data in the data set would probably improve the result quality of the envelope prediction. This could probably improve the error percentage which is most synonymous with the critical point prediction.

## Bibliography

Al-Farhan, F and Ayala L.: "Optimization of Surface Separation Conditions for natural Gases Using Artificial Using Artificial Intelligence," Journal of Petroleum Science and Engineering, v.53, p. 135-147, August 2006.

Alfradique, M. F. and Castier, M.: "Calculation of Phase Equilibrium of Natural Gases with the Peng-Robinson and PC-SAFT Equations of State," Oil and Gas Science and Technology, v. 62, p. 62, p. 707-714, 2007.

Asselineau, L., Bogdanic, G., Vidal, J.: "A Versatile Algorithm for Calculating Vapor-Liquid Equilibria," Fluid Phase Equilibria, v. 3, p. 273-290, 1979.

Ayala, L. F. and Ertekin, T.: "Neuro-Simulation Analysis of Pressure Maintenance Operations in Gas Condensate Reservoirs," Journal of Petroleum Science and Engineering, v. 58, p. 207-226, 2007.

Mann III, Austin W.: "Intelligent Design of Natural Gas Storage Facilities" M.Sc. Thesis, The Pennsylvania State University, University Park, 2007.

Belue, L. M., and Bauer, K. W.: "Determining Input Features for Multilayer Preceptrons," Neurocomputing, v. 7, n.2, p. 111-121, 1995.

Briones, M. F., Corpoven, S. A. Rojas, G. A., Moreno, J. A. and Martinez E. R.:

“Applications of Neural Networks in the Prediction of Reservoir Hydrocarbon Mixture Composition from Production Data”, paper SPE 38855, Presented at the Annual Technical Conference and Exhibition held in New Orleans, LA, USA, 25-28 September 1994.

Danesh, A.: "PVT and Phase Behavior of Petroleum Reservoir Fluids," Elsevier, Second Edition p. 221-234, 2001.

Demuth, H. and Beale, M.: "Neural Network Toolbox for Use with Matlab©," User's Guide, v.4, The MathWorks, 2007.

Etter, D. O and Kay, W. B.: "Critical Properties of Mixture of Normal Paraffin Hydrocarbons, "Journal of Chemical Engineering Data, v. 1, p 409-414, 1961

Fazlali, A., Modarress, H. and Monsoori, G. A.: "Phase Behavior of Complex Fluids," Fluid Phase Equilibria, v. 179, p. 297-317, 2001.

Firoozabadi, A., Hoteit, H. and Santiso, E.: "An Efficient and Robust Algorithm for the Calculation of Gas-Liquid Critical Point of Multicomponent Petroleum Fluids," Fluid Phase Equilibria, v. 241, p. 186-195, 2006.

González, A., Barrufet, M.A. and Startzman, R.: "Improved neural-network model predicts dew point pressure of retrograde gases," *Journal of Petroleum Science and Engineering*, v. 37, p. 183-194, 2003.

Grieves, R. B. and Thodos, G.: "Cricodentherm and Cricondenbar Pressures of Multicomponent Hydrocarbon Mixtures," *SPE Journal*, v. 4, p.240-246, 1964. SPE 865.

Grieves, R. B. and Thodos, G.: " Cricodentherm and Cricondenbar Temperature of Multicomponent Hydrocarbon Mixtures" *SPE Journal*, v. 3, p.287-292, 1963. SPE 612.

Manafi, H., Mansoori G. A. and Ghotbi, S.: " Phase Behavior Prediction of Petroleum Fluids with Minimum Characterizations Data," *Journal of Petroleum of Science and Engineering*, v. 22, p. 67-93, 1999.

Michelsen, M. L.: "Calculation of Phase Envelopes and Critical Points for Multicomponent Mixtures", *Fluid Phase Equilibria*, v. 4, p. 1-10, 1980.

Michelsen, M. L.: "The Isothermal Flash Problem. Part I. Stability", *Fluid Phase Equilibria*, v. 9, p. 1-19, 1982.

Michelsen, M. L.: "The Isothermal Flash Problem. Part II. Phase-Split Calculation," Fluid Phase Equilibria, v. 9, p. 21-40, 1982.

Michelsen, M. L.: "Calculation of Critical Points and Phase Boundaries in the Critical Region", Fluid Phase Equilibria, v. 16, p. 57-76, 1984.

Michelsen, M. L.: "Saturation point Calculations", Fluid Phase Equilibria, v. 23, p. 181-192, 1985.

Ming-Jer L., and Jui-Tang, C.: "fluid Property Predictions with the Aid of Neural Networks" Industrial and Engineering Chemistry Research, v. 32, p. 995-997, 1993.

Nichita, D. V.: "Calculations of Critical Points Using a Reduction Method," Fluid Phase Equilibria, v. 1228, p. 223-231, 2005.

Nichita, D. V.: "Phase Envelope Construction for Mixtures with Many Components," Energy and Fuels, v. 22, p. 488-495, 2008.

Pedersen, Karen Schou and Christensen Peter, L.: "Phase Behavior of Petroleum Reservoir Fluids ", v. 1, p. 1-11.

- Peng, D.Y. and Robinson, D.B.: "A New Two-Constant Equation of State," *Industrial and Engineering Chemistry Fundamentals*, v.15, p.59-64, 1976.
- Poling B.E. and Ziervogel R.G.: "A Simple Method for Constructing Phase Envelopes for Multicomponent Mixtures," *Fluid Phase Equilibria*, v. 11, p. 127-135, 1983.
- Silver, E. D and Thodos George.: "Cricondentherms and Cricondenbars. Their Prediction for Binary hydrocarbon Systems", *Industrial and Engineering Chemistry Fundamentals*, v. 1, p. 299-303, 1962
- Spencer, F. C. and Daubert, T. E.: "A Critical Evaluation of Methods for the Prediction of Critical Properties of Hydrocarbon," *AIChE Journal*, v. 19, p.482-485, 1973.
- Stergiou, C. and Dimitrios, S.: "Neural Networks" [www.doc.ic.ac.uk](http://www.doc.ic.ac.uk).
- Taraf, R., Behbahani, R., and Moshfeghian, M.: "Direct Prediction of Cricondentherm and Cricondenbar Coordinates of Natural Gas Mixtures Using Cubic Equation of State", *International Journal of Thermophysics*, v. 28, p. 1954-1967, 2008.
- Yau-Kan, Li., and Nghiem L. X.: "The Development of a General Phase Envelope Construction Algorithm for Reservoir Fluid Studies," SPE 11198, Presented at the Annual Fall Technical Conference and Exhibition held in New Orleans, LA, USA, 26-29 September 1982.

Yilmaz, S., Demircioglu C., and Akin S.: "Application of Neural Networks to Optimum Bit Selection", Computers and Geosciences, v. 28, p. 261-269, 2002.

## Appendix A

### Stage 1 ANN MATLAB Code Cricondenbar

```
close all;
clear all;
format long;
%%
%%%Load the Input files for the testing and training of the network for
%%% and the Output data set....
load INP.txt;

load CriBar.txt;

load TestnIn.txt;

load CribTestOut.txt;
%%
%% Transpose the matrix into the appropriate format..
P= INP;
P = P';
T= CriBar;
T= T';
p1 = TestnIn;
p1 = p1';
t1 = CribTestOut;
t1 = t1';
%%
%%%Determine the size of the matrix in each data set.....
[m1,n1] = size (p1);

[m,n] = size (P);

[mo,no] = size (T);
%%
%%
%%% Normalizing the matrix in the proper intervals [-1, 1]
[Pn,ps] = mapminmax(P,-1,1);
[Tn,ts] = mapminmax(T,-1,1);
pn=mapminmax('apply',p1,ps);
tn=mapminmax('apply',t1,ts);
%%
%%% defining the into the format of the code
trainP=Pn;
trainT=Tn;
testP=pn;
testT=tn;

%%
```

```

%% training the neural network for the phase envelope values
net = newcf (minmax(Pn), [15 15 mo], {'tansig' 'tansig' 'purelin'},
'traincgf','learngdm','mse') ;
%%
%%
%%% Setting the Network parameters and goals
%%% as best suited for each individual network
net.trainParam.shows=5;          %%Epochs between displays
net.trainParam.goal=0.00001;    %%Performance goal
net.trainParam.epochs=6500;    %%Number of iterations for training
net.trainParam.max_fail=100000; %%Maximum validation failures
net.trainParam.mem_reduc=5;     %%Factor to use for memory/speed
tradeoff
net=init(net);
%%
% Start training network for both input trainP and output trainT

[net,tr]= train(net,trainP,trainT);
% simulating the input using the matrix pn
AAA = sim (net,trainP);
% denormalizing the input
AA = mapminmax('reverse', AAA,ts);
% denormalizing the targets
BBB =sim(net,testP);
BB =  mapminmax('reverse',BBB,ts);

t=T;

%%
%%% plots which is given by the \
%%% the network prediction and training
% Error calculation
errortrainingA=((AA(1,:)-(t(1,:)))./t(1,:)).*100;    %Training error for
Cricondenbar Reduced Pressure
errortrainingB=((AA(2,:)-(t(2,:)))./t(2,:)).*100;    %Training error for
Cricondenbar Reduced temperature

errortestingA=((BB(1,:)-(t1(1,:)))./t1(1,:)).*100;   %Testing error for
Cricondenbar Reduced Pressure
errortestingB=((BB(2,:)-(t1(2,:)))./t1(2,:)).*100;   %Testing error for
Cricondenbar Reduced temperature

X=[1:1:n];
XX=[1:1:n1];
binmax=10;
nbins=-binmax:binmax/10:binmax;
%%%%%%%%%%%%%%%%%%%%%%%%%%%%%%%%%%%%%%%%%%%%%%%%%%%%%%%%%%%%%%%%%%%%%%%%
%%%%%%%%
%Plots of training datas
%%%%%%%%%%%%%%%%%%%%%%%%%%%%%%%%%%%%%%%%%%%%%%%%%%%%%%%%%%%%%%%%%%%%%%%%
%%%%%%%%
figure (2)
filename = 'CriBar Pr training';
subplot (2,2,1, 'align');

```

```

plot (X,t(1,:), 'ko');
xlim ([0 n]);
hold on
grid on
plot (X,AA(1,:), '-r*');
ylabel('Pr for Cricondenbar');
xlabel('Data set');
h =legend ('Actual', 'Ann values', 'location', 'NorthEast');
title (filename);
xlim ([0 n]);
ylim ([0 20]);

subplot (2,2,2, 'align');
plot (XX,t1(1,:), 'ro-');
grid on
hold on
plot (XX,BB(1,:), 'b*--');
xlim([0 n]);
ylabel ('Pr testing for cricondenbar');
xlabel('data set');
h =legend ('Actual', 'Ann values', 'location', 'NorthEast');
xlim([0 n]);
ylim([0 20]);

subplot (2,2,3, 'align');
plot (X,t(2,:), 'ko');
hold on
grid on
plot (X,AA(2,:), '-r*');
ylabel('Tr for Cricondenbar');
xlabel('Data set');
legend ('Actual', 'Ann values', 'location', 'NorthEast');
% title (filename);
xlim ([0 n]);
ylim ([0 20]);

subplot (2,2,4, 'align');
plot (XX,t1(2,:), 'ro-');
grid on
hold on
plot (XX,BB(2,:), 'b*--');
xlim([0 n]);
ylabel ('Tr testing for cricondenbar');
xlabel('data set');
h =legend ('Actual', 'Ann values', 'location', 'NorthEast');
xlim([0 n]);
ylim([0 20]);

figure(3)
subplot (2,2,1, 'align');
plot (X,errortrainingA, 'k+');
grid on
hold on
ylabel('error % TrainingPr for Cricondenbar');

```

```

xlabel('Data set');
xlim ([0 n]);
ylim ([0 20]);

subplot (2,2,2, 'align');
plot (XX,errortestingA, 'k+');
grid on
hold on
ylabel('error % TestingPr for Cricondenbar');
xlabel('Data set');
xlim ([0 n]);
ylim ([0 20]);

subplot (2,2,3, 'align');
plot (X,errortrainingB, 'k+');
grid on
hold on
ylabel('error % traingTr for Cricondenbar');
xlabel('Data set');
xlim ([0 n]);
ylim ([0 20]);

subplot (2,2,4, 'align');
plot (XX,errortestingB, 'k+');
grid on
hold on
ylabel('error% testingTr for Cricondenbar');
xlabel('Data set');
xlim ([0 n]);
ylim ([0 20]);

%%%%%%%%%%%%%%%%%%%%%%%%%%%%%%%%%%%%%%%%%%%%%%%%%%%%%%%%%%%%%%%%%%%%%%%%
%Plots of histogram and cross plots
%%%%%%%%%%%%%%%%%%%%%%%%%%%%%%%%%%%%%%%%%%%%%%%%%%%%%%%%%%%%%%%%%%%%%%%%
% %binmax=5;
% nbins=-binmax:binmax/10:binmax;
% errortestingA
% % %plots
figure (4)
subplot(2,2,1)
hist(errortrainingA,nbins)
h = findobj(gca, 'Type', 'patch');
set(h, 'FaceColor', 'r', 'EdgeColor', 'w')
xlim([-binmax binmax]);
title('Training Pr for CriB* Histogram')

subplot(2,2,2)
hist(errortestingA,nbins)
h = findobj(gca, 'Type', 'patch');
set(h, 'FaceColor', 'r', 'EdgeColor', 'w')
xlim([-binmax binmax]);

```

```

title('Testing Pr for CriB* Histogram')
%%%%%%%%%%%%%%%%%%%%%%%%%%%%%%%%%%%%%%%%%%%%%%%%%%%%%%%%%%%%%%%%%%%%%%%%

subplot(2,2,3)
hist(errortrainingB,nbins)
h = findobj(gca,'Type','patch');
set(h,'FaceColor','r','EdgeColor','w')
xlim([-binmax binmax]);
title('Training Tr for CriB* Histogram')

subplot(2,2,4)
hist(errortestingB,nbins)
h = findobj(gca,'Type','patch');
set(h,'FaceColor','r','EdgeColor','w')
xlim([-binmax binmax]);
title('Testing Tr for CriB* Histogram')
%%%%%%%%%%%%%%%%%%%%%%%%%%%%%%%%%%%%%%%%%%%%%%%%%%%%%%%%%%%%%%%%%%%%%%%%

%%%%%%%%%%%%%%%%%%%%%%%%%%%%%%%%%%%%%%%%%%%%%%%%%%%%%%%%%%%%%%%%%%%%%%%%

figure (5)
subplot(2,2,1)
plot(t(1,:),AA(1:,:), 'bo')
grid on
hold on
x = 0.55:1:14.0;
y = x;
plot(x,y, '-k')
xlim([1.2 2.6]);
ylim([1.2 2.6]);
xlabel('Actual')
ylabel('Predicted')
title('Training CriconB Pr* Crossplot')

subplot(2,2,2)
plot(t1(1,:),BB(1:,:), 'bo')
grid on
hold on
x = -5.18:1:11.1;
y = x;
plot(x,y, '-k')
xlim([1.4 2.4]);
ylim([1.4 2.4]);
xlabel('Actual')
ylabel('Predicted')
title('Testing CriconB Pr* Crossplot')

subplot(2,2,3)
plot(t(2,:),AA(2:,:), 'bo')
grid on
hold on

```

```
x = 0.55:1:14.0;
y = x;
plot(x,y, '-k')
xlim([2.0 10.0]);
ylim([2.0 10.0]);
xlabel('Actual')
ylabel('Predicted')
title('Training CriconB Tr* Crossplot')

subplot(2,2,4)
plot(t1(2,:),BB(2,:), 'bo')
grid on
hold on
x = -5.18:1:11.1;
y = x;
plot(x,y, '-k')
xlim([2.0 10.0]);
ylim([2.0 10.0]);
xlabel('Actual')
ylabel('Predicted')
title('Testing CriconB Tr* Crossplot')

figure (6)
plot (CribTestOut(:,1),CribTestOut(:,2), 'ob');
hold on
plot (CriBar(:,1),CriBar(:,2), 'or');
```

N:B Same program was used for the Cricondentherm and Critical Calculations only difference is the files which was loaded.

## Appendix B

### Phase Envelope Code for MATLAB Stage Two

```

%%
close all;
clear all;
%%
%%%Load the Input files for the testing and training of the network for
%%% and the Output data set....
load TrainIn.txt;
load TrainOut.txt;
load TestIn.txt;
load TestOut.txt;
%%
%% Transpose the matrix into the appropriate format..
P= TrainIn;
P = P';
T= TrainOut;
T= T';
p=TestIn;
p=p';
t1=TestOut;
t1=t1';
%%
%%%Determine the size of the matrix in each data set.....
[m,n] = size (P);
[mo,no] = size (T);
[m1,n1] = size (p);
%%
%%% Normalizing the matrix in the proper intervals [-1, 1]
[Pn,ps] = mapminmax(P,-1,1);
[Tn,ts] = mapminmax(T,-1,1);
pn=mapminmax('apply',p,ps);

trainP=Pn;
trainT=Tn;
testP=pn;
testT=t1;

%% training the neural network for the phase envelope values
net = newcf (minmax(Pn), [20 15 15 mo], {'tansig' 'tansig' 'tansig'
'purelin'}, 'traincgf','learngdm','mse') ;
%%
%%
%%% Seting the Network parameters and goals
%%% as best suited for each individual iterations

net.trainParam.shows=5;          %%Epochs between displays
net.trainParam.goal=0.0001;      %%Performance goal
net.trainParam.epochs=10000;     %%Number of iterations for training
net.trainParam.max_fail=1000;    %%Maximum validation failures

```

```

net.trainParam.mem_reduc=5;    %%Factor to use for memory/speed
tradeoff
net=init(net);

%% training network Starts.
    %% Training actual network with Just Input trainP and Output trainT
[net,tr]= train(net,trainP,trainT);

% plotperf(TR,goal,name,epoch)
plotperform(tr);
AAA = sim (net,trainP);

% denormalizing the input
AA = mapminmax('reverse', AAA,ts);

% mapminmax
BBB =sim(net,testP);
BB = mapminmax('reverse',BBB,ts);

t=T;
%%
% Error calculation
errortrainingA=((AA(1,:)-(t(1,:)))./t(1,:)).*100;    %Training error for
Cricondenbar Normalized temperaturebuknow sa
errortrainingB=((AA(2,:)-(t(2,:)))./t(2,:)).*100;    %Training error for
Cricondenbar Normalized Pressure
errortrainingC=((AA(3,:)-(t(3,:)))./t(3,:)).*100;    %Training error for
Cricondentherm Normalized temperature
errortrainingD=((AA(4,:)-(t(4,:)))./t(4,:)).*100;    %Training error for
Cricondentherm Normalized Pressure
errortrainingE=((AA(5,:)-(t(5,:)))./t(5,:)).*100;    %Training error for
critical Point Normalized temperature
errortrainingF=((AA(6,:)-(t(6,:)))./t(6,:)).*100;    %Training error for
critical Point Normalized Pressure
errortestingA=((BB(1,:)-(t1(1,:)))./t1(1,:)).*100;    %Testing error for
Cricondenbar Normalized temperature
errortestingB=((BB(2,:)-(t1(2,:)))./t1(2,:)).*100;    %Testing error for
Cricondenbar Normalized Pressure
errortestingC=((BB(3,:)-(t1(3,:)))./t1(3,:)).*100;    %Testing error for
Cricondentherm Normalized temperature
errortestingD=((BB(4,:)-(t1(4,:)))./t1(4,:)).*100;    %Testing error for
Cricondentherm Normalized Pressure
errortestingE=((BB(5,:)-(t1(5,:)))./t1(5,:)).*100;    %Testing error for
Critical Point Normalized temperature
errortestingF=((BB(6,:)-(t1(6,:)))./t1(6,:)).*100;    %Testing error for
Critical Point Normalized Pressure

X=[1:1:n];
XX=[1:1:n1];

```

```

binmax=10;
nbins=-binmax:binmax/10:binmax;
%%%%%%%%%%%%%%%%%%%%%%%%%%%%%%%%%%%%%%%%%%%%%%%%%%%%%%%%%%%%%%%%%%%%%%%%
%%%%%%%%%%%%%%%%%%%%%%%%%%%%%%%%%%%%%%%%%%%%%%%%%%%%%%%%%%%%%%%%%%%%%%%%
%Plots of training datas
%%%%%%%%%%%%%%%%%%%%%%%%%%%%%%%%%%%%%%%%%%%%%%%%%%%%%%%%%%%%%%%%%%%%%%%%
%%%%%%%%%%%%%%%%%%%%%%%%%%%%%%%%%%%%%%%%%%%%%%%%%%%%%%%%%%%%%%%%%%%%%%%%
figure (2)
subplot (3,2,1, 'align');
plot (X,errortrainingA,'k+');
grid on
hold on
ylabel('error % T for Cricondenbar');
xlabel('Data set');
xlim ([0 n]);
ylim ([-10 20]);

subplot (3,2,2, 'align');
plot (XX,errortestingA,'k+');
grid on
hold on
ylabel('error % TestingT for Cricondenbar');
xlabel('Data set');
xlim ([0 n1]);
ylim ([-10 20]);

subplot(3,2,3)
hist(errortrainingA,nbins)
h = findobj(gca,'Type','patch');
set(h,'FaceColor','r','EdgeColor','w')
xlim([-binmax binmax]);
title('Training T for CriB* Histogram')

subplot(3,2,4)
hist(errortestingA,nbins)
h = findobj(gca,'Type','patch');
set(h,'FaceColor','r','EdgeColor','w')
xlim([-binmax binmax]);
title('Testing T for CriB* Histogram')
%%%%%%%%%%%%%%%%%%%%%%%%%%%%%%%%%%%%%%%%%%%%%%%%%%%%%%%%%%%%%%%%%%%%%%%%
subplot(3,2,5)
plot(t(1,:),AA(1:,:),'bo')
grid on
hold on
x = 0.55:1:14.0;
y = x;
plot(x,y,'-k')
xlim([1.2 2.6]);
ylim([1.2 2.6]);
xlabel('Actual')
ylabel('Predicted')
title('Training CriconB T* Crossplot')

subplot(3,2,6)

```

```

plot(t1(1,:),BB(1:,:), 'bo')
grid on
hold on
x = -5.18:1:11.1;
y = x;
plot(x,y, '-k')
xlim([1.4 2.4]);
ylim([1.4 2.4]);
xlabel('Actual')
ylabel('Predicted')
title('Testing CriconB T* Crossplot')

%%
%%
figure(3)
subplot (3,2,1, 'align');
plot (X,errortrainingB, 'k+');
grid on
hold on
ylabel('error % P for Cricondenbar');
xlabel('Data set');
xlim ([0 n]);
ylim ([-10 20]);

subplot (3,2,2, 'align');
plot (XX,errortestingB, 'k+');
grid on
hold on
ylabel('error% testingP for Cricondenbar');
xlabel('Data set');
xlim ([0 n1]);
ylim ([-10 20]);

subplot(3,2,3)
hist(errortrainingB,nbins)
h = findobj(gca, 'Type', 'patch');
set(h, 'FaceColor', 'r', 'EdgeColor', 'w')
xlim([-binmax binmax]);
title('Training P for CriB* Histogram')

subplot(3,2,4)
hist(errortestingB,nbins)
h = findobj(gca, 'Type', 'patch');
set(h, 'FaceColor', 'r', 'EdgeColor', 'w')
xlim([-binmax binmax]);
title('Testing Pr for CriB* Histogram')

subplot(3,2,5)
plot(t(2,:),AA(2:,:), 'bo')
grid on
hold on
x = 0.55:1:14.0;
y = x;
plot(x,y, '-k')

```

```

xlim([2.0 10.0]);
ylim([2.0 10.0]);
xlabel('Actual')
ylabel('Predicted')
title('Training CriconB P* Crossplot')

subplot(3,2,6)
plot(t1(2,:),BB(2,:), 'bo')
grid on
hold on
x = -5.18:1:11.1;
y = x;
plot(x,y, '-k')
xlim([2.0 10.0]);
ylim([2.0 10.0]);
xlabel('Actual')
ylabel('Predicted')
title('Testing CriconB P* Crossplot')

figure(4)
subplot (3,2,1, 'align');
plot (X,errortrainingC, 'k+');
grid on
hold on
ylabel('error % T for Critherm');
xlabel('Data set');
xlim ([0 n]);
ylim ([-10 20]);

subplot (3,2,2, 'align');
plot (XX,errortestingC, 'k+');
grid on
hold on
ylabel('error % TestingT for Critherm');
xlabel('Data set');
xlim ([0 n1]);
ylim ([-10 20]);

subplot(3,2,3)
hist(errortrainingC,nbins)
h = findobj(gca, 'Type', 'patch');
set(h, 'FaceColor', 'r', 'EdgeColor', 'w')
xlim([-binmax binmax]);
title('Training T for CriConTherm* Histogram')

subplot(3,2,4)
hist(errortestingC,nbins)
h = findobj(gca, 'Type', 'patch');
set(h, 'FaceColor', 'r', 'EdgeColor', 'w')
xlim([-binmax binmax]);
title('Testing T for CriTherm* Histogram')

subplot(3,2,5)

```

```

plot(t(3,:),AA(3:), 'bo')
grid on
hold on
x = 0.55:1:14.0;
y = x;
plot(x,y, '-k')
xlim([1.50 3.0]);
ylim([1.50 3.0]);
xlabel('Actual')
ylabel('Predicted')
title('Training CriConTherm T* Crossplot')

subplot(3,2,6)
plot(t1(3,:),BB(3:), 'bo')
grid on
hold on
x = -5.18:1:11.1;
y = x;
plot(x,y, '-k')
xlim([1.50 3.0]);
ylim([1.50 3.0]);
xlabel('Actual')
ylabel('Predicted')
title('Testing CriConTherm T* Crossplot')

figure (5)
subplot (3,2,1, 'align');
plot (X,errortrainingD, 'k+');
grid on
hold on
ylabel('error % P for Critherm');
xlabel('Data set');
xlim ([0 n]);
ylim ([-10 20]);

subplot (3,2,2, 'align');
plot (XX,errortestingD, 'k+');
grid on
hold on
ylabel('error% testingP for Critherm');
xlabel('Data set');
xlim ([0 n1]);
ylim ([-10 20]);

subplot(3,2,3)
hist(errortrainingD,nbins)
h = findobj(gca, 'Type', 'patch');
set(h, 'FaceColor', 'r', 'EdgeColor', 'w')
xlim([-binmax binmax]);
title('Training P for CriTherm* Histogram')

subplot(3,2,4)
hist(errortestingD,nbins)

```

```

h = findobj(gca,'Type','patch');
set(h,'FaceColor','r','EdgeColor','w')
xlim([-binmax binmax]);
title('Testing P for CriTherm* Histogram')

subplot(3,2,5)
plot(t(4,:),AA(4:,:), 'bo')
grid on
hold on
x = 0.55:1:14.0;
y = x;
plot(x,y, '-k')
xlim([0.55 3.0]);
ylim([0.55 3.0]);
xlabel('Actual')
ylabel('Predicted')
title('Training CriConTherm P* Crossplot')

subplot(3,2,6)
plot(t1(4,:),BB(4:,:), 'bo')
grid on
hold on
x = -5.18:1:11.1;
y = x;
plot(x,y, '-k')
xlim([0.55 3.0]);
ylim([0.55 3.0]);
xlabel('Actual')
ylabel('Predicted')
title('Testing CriConTherm P* Crossplot')

figure (6)
subplot (3,2,1, 'align');
plot (X,errortrainingE, 'k+');
grid on
hold on
ylabel('error % T for Critical');
xlabel('Data set');
xlim ([0 n]);
ylim ([-10 20]);

subplot (3,2,2, 'align');
plot (XX,errortestingE, 'k+');
grid on
hold on
ylabel('error % TestingT for Critical');
xlabel('Data set');
xlim ([0 n1]);
ylim ([-10 10]);

subplot(3,2,3)
hist(errortrainingE,nbins)
h = findobj(gca,'Type','patch');

```

```

set(h, 'FaceColor', 'r', 'EdgeColor', 'w')
xlim([-binmax binmax]);
title('Training T for Cri* Histogram')

subplot(3,2,4)
hist(errortestingE,nbins)
h = findobj(gca, 'Type', 'patch');
set(h, 'FaceColor', 'r', 'EdgeColor', 'w')
xlim([-binmax binmax]);
title('Testing T for Cri* Histogram')

subplot(3,2,5)
plot(t(5,:),AA(5:,:), 'bo')
grid on
hold on
x = 0.55:1:14.0;
y = x;
plot(x,y, '-k')
xlim([0.55 3.0]);
ylim([0.55 3.0]);
xlabel('Actual')
ylabel('Predicted')
title('Training Critical T_N* Crossplot')

subplot(3,2,6)
plot(t1(5,:),BB(5:,:), 'bo')
grid on
hold on
x = -5.18:1:15.1;
y = x;
plot(x,y, '-k')
xlim([0.55 3.0]);
ylim([0.55 3.0]);
xlabel('Actual')
ylabel('Predicted')
title('Testing Critical T_N* Crossplot')

%%%%%%%%%%%%%%
figure (7)
subplot (3,2,1, 'align');
plot (X,errortrainingF, 'k+');
grid on
hold on
ylabel('error % P for Critical');
xlabel('Data set');
xlim ([0 n]);
ylim ([-10 20]);

subplot (3,2,2, 'align');
plot (XX,errortestingF, 'k+');
grid on
hold on
ylabel('error% testingP for Critical');
xlabel('Data set');

```

```

xlim ([0 n1]);
ylim ([-10 10]);
%%%%%%%%%%
subplot(3,2,3)
hist(errortrainingF,nbins)
h = findobj(gca,'Type','patch');
set(h,'FaceColor','r','EdgeColor','w')
xlim([-binmax binmax]);
title('Training P for Cri* Histogram')

subplot(3,2,4)
hist(errortestingF,nbins)
h = findobj(gca,'Type','patch');
set(h,'FaceColor','r','EdgeColor','w')
xlim([-binmax binmax]);
title('Testing P for Cri* Histogram')

subplot(3,2,5)
plot(t(6,:),AA(6,:),'bo')
grid on
hold on
x = 0.55:1:12.0;
y = x;
plot(x,y,'-k')
xlim([0.55 12.0]);
ylim([0.55 12.0]);
xlabel('Actual')
ylabel('Predicted')
title('Training Critical P_N* Crossplot')

subplot(3,2,6)
plot(t1(6,:),BB(6,:),'bo')
grid on
hold on
x = -5.18:1:12.0;
y = x;
plot(x,y,'-k')
xlim([0.55 12.0]);
ylim([0.55 12.0]);
xlabel('Actual')
ylabel('Predicted')
title('Testing Critical P_N* Crossplot')

%=====
=====

%=====
=====

%% Get relevancies
% num. of neurons in 1st (input) layer

```

```
ni = net.layers{1}.size;
% num. of input elements
nj = net.inputs{1}.size;

% input weights MATRIX for
% ith layer, jth input source
% ANN.IW{i,j}
% assign absolute values of input weights
% for 1st (input) layer and 1st (this case only) input source

s = abs(net.IW{1,1});

for j = 1:nj
% outer loop: over input elements
    CS(j) = 0;
    for i = 1:ni
% inner loop: over 1st (input) layer neuron weights
        CS(j) = CS(j) + s(i,j);
    end
end

sum = 0;
for k = 1:nj
    sum = sum + CS(k);
end
```

```
percentCS = CS./sum * 100;
```

```
save%('')
```

```
%=====
```

```
%% FIGURE: Relevancies
```

```
%=====
```

```
figure(8);
```

```
name = ('Relevancies');
```

```
barh(CS,0.2,'k');
```

```
title('Input Relevancies');
```

```
xlabel('Relevancy');
```

```
set(gca,'YTickLabel',{...
```

```
    'Hydrogen Sulfide H2S';...
```

```
    'Carbondioxide CO2';...
```

```
    'Nitrogen N2';...
```

```
    'Methane C1';...
```

```
    'Ethane C2';...
```

```
    'Propane C3';...
```

```
    'Butane C4';...
```

```
    'Pentane C5';...
```

```
    'Hexane C6';...
```

```

    'Heptanes C7+' ; ...

    'Molecular Weight C7+' ; ...

    'Specific Gravity C7+' ; ...
    })

%   print ('-f','-dmeta',filename);

%   print ('-f','-depsc','-tiff',filename);
%
%   print ('-f','-r300','-djpeg100',filename);
%
%   clf('reset')

```

figure (9)

```

filename = ('Relevancies(percent)');

barh(percentCS,0.2,'k')

title('Input Relevancies (%)');

xlabel('Relevancy (%)');

set(gca, 'YTickLabel', { ...

    'Hydrogen Sulfide H2S' ; ...

    'Carbondioxide CO2' ; ...

    'Nitrogen N2' ; ...

    'Methane C1' ; ...

    'Ethane C2' ; ...

    'Propane C3' ; ...

    'Butane C4' ; ...

    'Pentane C5' ; ...

```

```
'Hexane C6';...  
  
'Heptanes C7+';...  
  
'Molecular Weight C7+';...  
  
'Specific Gravity C7+';...  
})  
  
% print ('-f','-dmeta',filename);  
  
% print ('-f','-depsec','-tiff',filename);  
  
% print ('-f','-r300','-djpeg100',filename);  
%  
% clf('reset')
```